Real-Time Tip Position Control of a Flexible Link Robot

A Thesis Submitted in Partial Fulfillment

of the Requirements for the Award of the Degree of

Master of Technology

in

Power Control & Drives

by

Abhisek Kumar Behera

Department of Electrical Engineering

National Institute of Technology Rourkela

June 2011

Real-Time Tip Position Control of a Flexible Link Robot

A Thesis Submitted in Partial Fulfillment

of the Requirements for the Award of the Degree of

Master of Technology

in

Power Control & Drives

by

Abhisek Kumar Behera

(209EE2159)

Under the supervision

of

Prof. Bidyadhar Subudhi

Prof. Sandip Ghosh

Department of Electrical Engineering

National Institute of Technology Rourkela

June 2011

ABSTRACT

Lightweight flexible robots are widely used in space applications due to their fast response and operation at high speed compared to conventional industrial rigid link robots. But the modeling and control of a flexible robot is more complex and difficult due to distributed structural flexibility. Further, a number of control complexities are encountered in case of flexible link robots such as non-minimum phase and under actuated behavior, non linear time varying and distributed parameter systems. Many control strategies have been proposed in the past, but most of the works have not considered the actuator dynamics and experimental validation of the modeling.

In this thesis, we consider the actuator dynamics is considered in modeling and also we have undertaken the experimental validation of the modeling. Tip positioning is the prime control objective of interest in many robotics applications. A tip feedback joint PD control has been proposed for tip positioning of the single link flexible robot. Gains of the controller have been obtained by using genetic algorithm and bacteria foraging optimization methods. By exploiting the above two evolutionary computing techniques for obtaining optimal gains good tip position control has been achieved together with good tracking control. The performances of the above two evolutionary computing tuned controller have been verified by both simulation and experiments.

Department of Electrical Engineering

National Institute of Technology Rourkela

Certificate

This is to certify that the Thesis entitled, "**Real-Time Tip Position Control of a Flexible Link Robot**" submitted by "**Abhisek Kumar Behera"** to the National Institute of Technology Rourkela is a bonafide research work carried out by him under our guidance and is worthy for the award of the degree of "**Master of Technology"** in Electrical Engineering specializing in "**Power Control and Drives"** from this institute. The embodiment of this thesis is not submitted in any other university and/or institute for the award of any degree or diploma to the best of our knowledge and belief.

Prof. Bidyadhar Subudhi
Professor and Head
Department of Electrical Engineering
Supervisor

Prof. Sandip Ghosh
Assistant Professor
Department of Electrical Engineering
Supervisor

Date:

Acknowledgements

There are many people who are associated with this project directly or indirectly whose help and timely suggestions are highly appreciable for completion of this project. First of all, I would like to thank my thesis supervisors Professors Bidyadhar Subudhi and Sandip Ghosh for their kind support and constant encouragements, valuable discussions which is highly commendable. Problem solving with careful observation by Professor Sandip Ghosh is unique which helped me a lot in my dissertation work and of course in due time. The discussion held with the friends and research scholars of control and robotics lab is worth to mention especially with Raja Rout, Srinibas Bhuyan, Jatin Kumar Pradhan and to my roommate Satyaranjan Jena.

My due thanks to Professors P. C. Panda, S. Rauta, A. K. Panda, K. B. Mohanty of the Electrical Engineering department for their course work which helped me in completing my dissertation work. Thanks to those who are also the part of this project whose names could have not been mentioned here. I highly acknowledge the financial support made by Ministry of Human Resource and Development so as to meet the expenses for study.

Lastly, I mention my indebtedness to my mother for her love and affection and especially her courage which made to believe myself.

Abhisek Kumar Behera

Contents

List of Figures

List of Tables

Chapter 1

Introduction to Flexible Link Robots

1.1 Introduction

Robots are widely used in many areas such as in industries, microsurgery, defense, space vehicles etc. in order to make the life of people more comfortable, safety and sophisticated. Initially these are massive in structure and their application was limited to only industrial purposes. Day by day due to advancement of modern technology, robots have become integral part of the development and progress of nation. Now they are used in the areas of specific interest starting from industry, biotech, research & development, defense, entertainment are name to few. However in modern days system miniature is the prime requirement in the design and compatibility to any systems. So research led to the development of lightweight structure robots which drew attention of many engineers for further development in the areas of robotics. These flexible robots are not only lighter than conventional rigid robots but they are also fast in response. In fact, in addition to these benefits they are associated with serious control problem of vibration. As the structure is flexible when it is actuated it vibrates with low frequency and it take some time to damp it out. Therefore the control problem for the flexible robot is more complex

than rigid link robots. Notwithstanding the interest in flexible structures is increased due to available of many advanced control techniques.

1.1.1 What is a flexible robot?

When the rigid links are replaced by lightweight links it is their inherent property that they undergo some damped vibration before it comes to the steady state. In contrast to this when rigid link robots are actuated they go to their final destination as a link the whole. However, if we move flexible link very slowly to its final position in case of a regulation problem or tracking to a very low frequency signal would result almost no or zero deflection. Therefore, it can be said that speed of operation which actually determine the tip vibration; higher the speed more seriously excited vibration and vice versa. At this we can define what flexibility is; "it is the property of the body by virtue of which the body vibrates with infinite modes of frequency at every point on the body when any bounded input make the body move from its position of rest". Quantitatively it can be said that flexibility is the measure of speed of operation. This will make sense if operation of flexible robot is understood from pictorial representation. Refer to Fig.1.1, link of the robotic system is initially at rest and when actuator is actuated to move the link through an angle θ it would move as a whole body to angle θ if it were a rigid link robot. However due to their structural flexibility, robot goes to final position but deforms from its steady state position and it come to steady state position after some time because of the damped vibration. Very interesting point to be noted here is that the deformation of the body is different at different points.

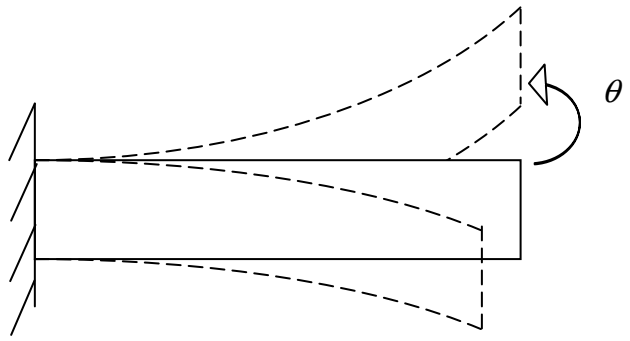

Fig. 1.1 Vibration of a flexible beam

For mathematical point of view we can say that the dynamics of the rigid link robot can be derived assuming the total mass to be concentrated at centre of gravity of the body hence dynamics of the robot would result in terms of differential equations. On contrary flexible robot position is not constant so rigid body analysis no more would be valid and so to represent the distributed nature of position along the beam partial differential equation is used. The control objective of the flexible link robot is also different from rigid link manipulator where vibration is suppressed within minimum time as soon as possible.

1.1.2 Why flexible robot?

Always fast response and weight are the requirements in the design and analysis in any system of interest. So these requirements necessitate the robot must have lightweight links which will enable them to be used in any area. In earlier days robots were primarily used in industrial automation sectors and their application in all other fields were limited. The application of robots especially in space were mainly constrained by their massive structures, bulky so flexible robot was an option for it and since then research on flexible structures control and modeling increased rapidly.

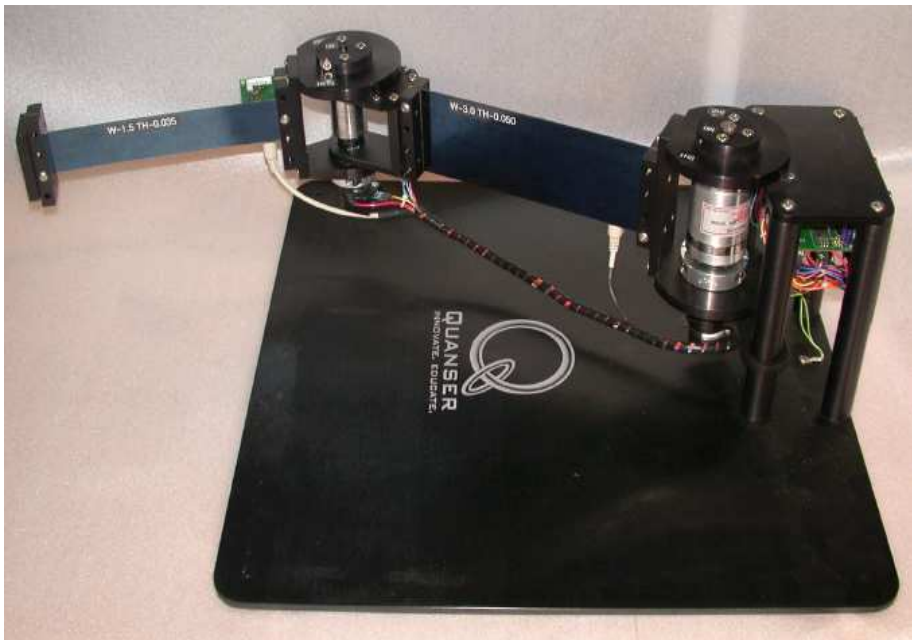

Fig. 1.2 Quanser two link flexible robot

Very peculiar problem in flexible robot is the modeling and control because in addition to tracking problem, vibration is more concerned to control engineers. Many universities around world have evinced interest in vibration suppression of flexible link robots due to wide application in defense, health care etc.

1.1.3 Advantages of flexible link robot

Flexible link robots possess many advantages over rigid link robots which are enumerated below.

- Lightweight structures
- Fast response
- High payload-to-arm weight ratio
- Low rated actuator
- Low power consumption

1.2 Review of some past works

Here we discuss some of the latest developments in the control strategies of flexible robot manipulator. The detailed discussion of flexible manipulator is given in chapter 2. There are numerous modeling techniques have been reported viz. lumped model [26], assumed mode method model [2]-[7], finite element method [9]-[10] [12], and implicit model [11]. However most of the works have not considered the dynamics of actuator and experimental verification of the model. Many control strategies developed for flexible manipulator control which concentrated on end point. Joint PD control [28], output feedback control law [17] is the basic control strategies are used for end point vibration suppression. However recent control techniques used neural network based inverse dynamic approach [18] and application of other soft computing tools are extensively seen.

1.3 Motivation

Many researchers have addressed on in the both modeling and control aspects of flexible link robot. The primary goal is to control the tip vibration as fast as possible. In addition to that many authors have reported the most crucial problems associated with flexible link robot are that non-minimum phase characteristic, non-collocated system and under actuated system [14] [18]. Design and analysis of controller for such systems is of very interest because the controller can be applicable to a wide class of system. Another important aspect of robotics is the instrumentation part. It is always desired to use sensors which can precisely reproduce the measurement signal because they are directly used in

the controller. In most robotic applications, the tip positioning/end-point control is crucial problem as the ultimate goal is to suppress the vibration very effectively.

1.4 Objectives

Numerous controllers have been designed for end point control of the robot starting from linear to nonlinear controller. Here in thesis we concentrate only on tip positioning problem of the flexible robot. The main objective is to reduce the complexities in the controller without sacrificing any performance measures. A simple joint PD tip feedback controller is designed where evolutionary techniques are used to tune the gains of the controller. The genetic algorithm is first used for tuning of gains of tip feedback controller and then simulation study is carried out for feasibility of the using these gains in real time experiments. Though the genetic algorithm is very simple, straightforward, we are interested to see further improvement by using bacteria foraging optimization (BFO). The concept of BFO came from swarming behavior of living creatures. Bacteria foraging optimization (BFO) is then used for tuning and a comparison analysis is done for tip performance of flexible robot.

1.5 Thesis organization

The work in thesis is organized into five chapters which are discussed below.

Chapter 1 provides a brief background of flexible robots, motivation and objectives of this thesis.

In chapter 2 we discuss the literatures citing modeling and control of flexible link manipulator.

The dynamics of the flexible link robot is derived in chapter 3. Both assumed mode method and finite element methods are employed in here. Different components such as sensors and actuators and principle of operation of this experimental setup are briefed in this chapter. This chapter ends with the open loop model validation using a bang-bang input voltage.

Chapter 4 describes the development and implementation of the proposed tip position controller. Both genetic algorithm and bacterial foraging optimization techniques are reviewed and exploited to optimal gains of the proposed controller. Simulation and experimental results are provided with discussions.

Chapter 5 concludes the work with suggestions for future work.

Chapter 2

Review on Modeling and Control of Flexible Robot Manipulators

2.1 Introduction

Initially research on flexible link robot manipulator was very limited due to its limited application. But their increase in importance due to successful applications and potential for future growth lead to further developments and contributions from researchers. Till date many developments both in modeling and control aspects of the robot have been reported in the peer reviewed papers. Still it is expected that the better controller could be designed for the control of flexible manipulator. A brief discussion of past works is given in subsequent section.

2.2 Literature survey

2.2.1 Review on modeling

Research on flexible manipulator started in late 80's. Modeling of the flexible robot has been reported using both assumed mode and finite element methods by many

researchers. A detailed study on the state-of-art development in the both modeling and control aspects is reviewed by Dwivedy and Eberhard [1]. Hastings and Book [2], Wang and Wei [3], Wang and Vidyasagar [4] studied single-link flexible manipulators using Lagrange's equation and the assumed mode method. Their work is supported by experimental analysis. In most of these cases joints were assumed to be stiff. The model for prismatic joints is reported in [5]-[6]. In [6], they also derived the non linear model of flexible link and then linearised it for controller design. A complete non linear model for single flexible link using assumed model is also carried out by Luca and Siciliano [7]. In their work they clearly reported about different modes of vibration and an inversion controller design based on that. They extended it to the two link flexible manipulator [8] and same work with payload variation is done by Ahmad *et al.* [25]. In [9]-[10] dynamical model for single link using finite element approach is proposed and compared with experimental results. They used bang-bang type of torque to study the dynamic response. However, explicitly represented truncated model analysis only first two finite modes as in case of assumed mode method or only two to three elements are considered as in the case of finite element so it result only the approximate result and even require precise measurements of signals. To avoid this, Ge, Lee and Zhu [11] proposed an implicit partial differential equation (PDE) model of single link flexible robot with design of a simple controller using train gauge measurement. The analysis for non linear model of flexible link using finite element is reported in [12]. Subudhi and Morris derived the dynamical model of a two link under actuated flexible joint and flexible link manipulator and designed a reduced-order controller based on singular perturbation method [13]. However, still there are developments in new techniques to model flexible link robot.

2.2.2 Review on control strategies

Vibration control of flexible robot is the research interest to many control engineers. Some earlier work of Geniele *et al*.[14] applied the linear controller developed from transfer function model for inner and outer stabilization of the flexible link is shown to yield better result. Moallem *et al*.[16] controlled the tip position of two link flexible robot using observer based inverse dynamics approach showing the tip vibration is effectively suppressed. An improved inversion based non linear controller is designed for position control for two link manipulator [15]. Conventional controller design like state feedback control law is implemented in 1989 [17]. Though many controllers are designed for flexible link for end point control they have to compromise between settling time and tip deflection (overshoot). In a way to provide faster response of tip position, Su & Khorasani [18] proposed neural network based inverse based controller, Subudhi & Morris [19] applied soft computing tools for tip control of flexible link. Comprehensive study of various controllers applicable to single link flexible manipulator for end point control [20] is given from practical point of view. Another new approach to end point control of flexible link is proposed by Ge *et al* [21] where genetic algorithm tuning of strain feedback controller [11] is studied by simulation studies. Recently many control strategies based on intelligent controller is addressed due to their successful implementation in many areas. In [22] an optimal intelligent controller is proposed with experimental analysis settling time significantly reduced. It is seen that the vibration of tip is sinusoidal nature indicates presence of some complex conjugate poles so a new controller called resonant controller which take care of these complex poles is designed [23]. Another technique of suppressing is commanding the actuator with input shaping

[24] proposed. Nevertheless the research is focused on the design some new controller that will perform better.

2.3 Summary

In this chapter development on flexible robot system is discussed briefly. Past works of flexible robot have been categorized into two sub sections; section 2.2.1 presents previous developments on modeling and section 2.2.2 overviews the control strategies.

Chapter 3

Dynamic Modeling of Flexible Link Robot System and Experimental Validation

3.1 Dynamics of single link flexible robot

Modeling of the flexible link robot poses great challenge to control engineers due to the inherent distributed structural flexibility. A lot of work citing exact modeling has been reported in the literatures. Both Assumed mode method (AMM) and Finite element method (FEM) modeling are employed to flexible robot system. An exact model is necessary for control of the system because the effectiveness of the controller depends on how exact is the model. Truncated model analysis is carried out by considering first two modes only. Although many papers reported the model of flexible robot but the actuator dynamics is not explicitly shown. So actuator dynamics is incorporated in the flexible link modeling for the complete representation of the model. Besides this; other models of the flexible link is proposed for energy based control design. The partial differential equation (PDE) model and lumped model are the few examples. These models don't explicitly address the dynamics behavior of the link hence control design based on model is expected to give unsatisfactory performance.

Here both AMM and FEM model are derived based on some assumption without losing any generality. The assumptions are as follow:

- Link is assumed to be of Euler-Bernoulli beam satisfying Euler-Bernoulli's beam equation.
- Have uniform mass density throughout the beam.
- Thickness of the beam is very small compared to the length.
- The link is placed horizontally making no consideration of gravitational factor in the model.
- Torsional vibration is neglected.

These assumptions make model derivation simple without introducing any appreciable error. The AMM method models the link deflection as combination of infinite number of separable modes of vibration subject to boundary conditions of Euler-Bernoulli's beam equation. The FEM models the link as a combination of finite number of elements connected serially subject to boundary conditions at each node. Moreover the deflection of the element in FEM is function of deflection at node but the mode concept is not present here.

3.1.1. Dynamics of actuator

The actuator which drives the link may be dc motor or ac motor. But dc motor is more common in robotics application. The actuator is placed at the hub of link connected through gear-box for safe operation of the link. The actuator configuration is shown in the figure 3.1. The control input to motor is fed from the amplifier and speed is reduced

by harmonic drive because it provides zero backlash and precise speed reduction is achieved by the harmonic drive.

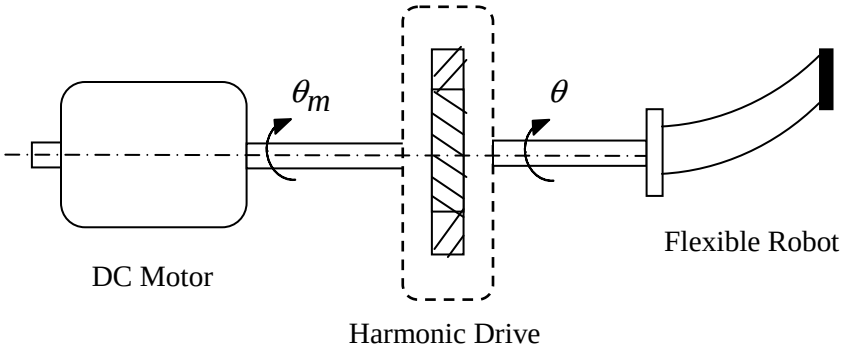

Fig. 3.1 Actuator configuration of the flexible link

Let θ_m and θ be the speed of motor at motor shaft and load shaft respectively. The motor rotates at very high speed which is reduced to a safe limit by gearbox. Gearboxes are associated with the backlash which is of no interest in robotics. Instead harmonic drive is used to effectively reduce the speed of the motor. Let us consider T_m, T_1, T_2 and T_L be the torque developed by the motor, torque at motor shaft, torque transmitted to the load and load torque respectively, J_m and J_L are the inertias of motor and load respectively, R_a, L_a, K_t, K_b and N_r are the armature resistance, inductance, motor torque constant, back emf constant and gear ratio respectively.

Applying KVL the voltage equation for the armature circuit can be written as

$$u = L_a \frac{di_a}{dt} + R_a i_a + e_b \quad \ldots\ldots\ldots\ldots\ldots\ldots\ldots\ldots\ldots\ldots \quad (3.1)$$

where $e_b = K_b\dot{\theta}_m$ is the back-emf generated in the armature circuit. Given the motor voltage u the current i_a flow through the armature circuit and develops electro-magnetic torque as $T_m = K_t i_a$. The torque developed is used to drive the flexible link through the speed reducer. Here harmonic drive is integrated with motor shaft and the flexible link is mounted on the harmonic drive. Since the speed of the motor is very high it is reduced to a safer value as

$$N_r = \frac{\theta_m}{\theta} = \frac{T_2}{T_1} \quad \text{..... (3.2)}$$

Referring to the Fig.3.1 the torque balance equation can be written as

$$T_m = J_m\ddot{\theta}_m + T_1 \quad \text{..... (3.3)}$$

and $$T_2 = J_L\ddot{\theta} + T_L \quad \text{..... (3.4)}$$

from equations (2.2)-(2.4), the load torque can be written as

$$T_L = N_r T_m - J_h\ddot{\theta} \quad \text{..... (3.5)}$$

where hub inertia of the robot $J_h = J_L + N_r^2 J_m$ is the total inertia referred to the load side of the motor. Substituting for T_m in equation (3.5), we get

$$T_L = N_r K_t i_a - J_h\ddot{\theta} \quad \text{..... (3.6)}$$

The equations (3.1) and (3.6) together completely describe the actuator dynamics of the robot.

3.1.2. Assumed mode method model

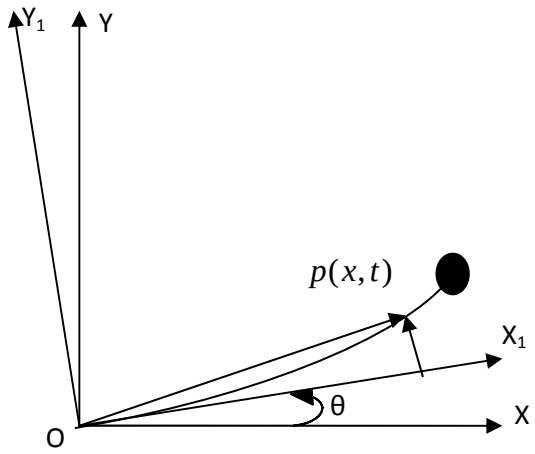

Fig. 3.2. Single link flexible robot

Consider a flexible link robot with body attached reference frame X_1OY_1 and fixed reference frame XOY. The different notations being used in subsequent sections are enumerated below:

L: Length of the flexible beam.

E: Young's modulus of elasticity of the material of the flexible beam.

I: Area moment of inertia of flexible beam.

ρ: Uniform mass density of the flexible beam.

M_L: Mass of the tip payload.

J_L: Inertia of the payload mass attached to the tip of the robot.

$y(x,t)$: Deflection of any point of the link measured from the body attached reference frame.

$p(x,t)$: Position of any point on the robot with respect to the fixed reference frame.

${}^{1}p_{1}(x,t)$: Position of any point with respect to body attached frame.

$r_1(L,t)$: Position of the tip of the robot with respect to fixed reference frame.

${}^{1}r_{1}(L,t)$: Position of the tip with respect to body attached reference frame.

When the link undergoes angular motion the tip of the robot vibrates which dies down with respect to time. Therefore the position of any point and the tip of the robot can be defined as

$$p(x,t) = A_R\,{}^{1}p_1(x,t) \quad \text{and} \quad r_1 = A_R\,{}^{1}r_1(L,t)$$

where $A_R = \begin{bmatrix} \cos\theta & -\sin\theta \\ \sin\theta & \cos\theta \end{bmatrix}$ the rotation matrix.

The dynamics of the robot is derived using Lagrange's equation of motion which requires the kinetic (KE) and potential energy (PE) of the system under consideration. By calculating the KE and PE the flexible link dynamics can be derived by satisfying the lagrangian the following equation:

$$\frac{d}{dt}\left(\frac{\partial L}{\partial \dot{q}}\right) - \frac{\partial L}{\partial q} = f \quad \text{..... (3.7)}$$

The KE of the system can be obtained as by deriving the KE of the link and tip separately. The KE of the link is given by

$$T_{link} = \frac{1}{2}\int_0^L \rho \dot{p}(x,t)^T \, \dot{p}(x,t)dx \quad \text{..... (3.8)}$$

Here the velocity of any point of link can be obtained as

$$\dot{p}(x,t) = \dot{A}_R{}^1 p_1(x,t) + A_R{}^1 \dot{p}_1(x,t)$$

Similarly the KE associated with the tip is given by

$$T_{tip} = \frac{1}{2} m_p \dot{r}_1^T \dot{r}_1 + \frac{1}{2} J_L (\dot{\theta} + \dot{y}_e')^2 \quad \text{..... (3.9)}$$

where $\dot{r}_1 = \dot{A}_R{}^1 r_1(L,t) + A_R{}^1 \dot{r}_1(L,t)$ is tip velocity.

and $y_e' = \left.\frac{\partial y(x,t)}{\partial x}\right|_{x=L}$ is the slope of the tip.

The PE of the system comprises of PE due to gravitation and elasticity property. However, owing to the horizontal configuration of the robot PE contributed by the gravity vanishes and elasticity of the body alone contribute toward the PE. So the PE of the link can be found as

$$U = \frac{1}{2}\int_0^L EI \left(\frac{\partial^2 y(x,t)}{\partial x^2} \right)^2 dx \quad \text{..... (3.10)}$$

The link dynamics can now be derived by employing equations (3.7)-(3.10). In fact the dynamics results in infinite dimensional distributed model due to distributed nature of

dynamical system which is in most cases avoided due to difficulty in controller design, clearly undefined system parameters. So truncated model analysis is preferred which approximate the infinite dimensional model to finite dimensional one without introducing any error.

The Euler-Bernoulli's beam equation representing the flexible link is given by:

$$EI\frac{\partial^4 y(x,t)}{\partial x^4}+\rho\frac{\partial^2 y(x,t)}{\partial t^2}=0 \quad \text{..... (3.11)}$$

To solve this equation proper boundary conditions must be known at prior both at clamped and free end. At clamped end the associated boundary conditions are given by

$$y(0,t)=0 \text{ and } y'(0,t)=0 \quad \text{..... (3.12)}$$

These two boundary conditions are explicitly understood that there is no deflection at clamped end. However, the payload mass attached to the tip contributes the inertia and moment, so the boundary condition at free end are represented as

$$EI\frac{\partial^2 y(x,t)}{\partial x^2}\bigg|_{x=L}=-J_L\frac{d^2}{dt^2}\left(\frac{\partial y(x,t)}{\partial x}\bigg|_{x=L}\right)$$

$$EI\frac{\partial^3 y(x,t)}{\partial x^3}\bigg|_{x=L}=M_L\frac{d^2}{dt^2}\left(y(x,t)|_{x=L}\right)$$

Considering the finite-dimensional modes of link flexibility the deflection can be written as

$$y(x,t) = \sum_{j=1}^{l} \phi_j(x)\delta_j(t) = \phi\delta \text{ ..... (3.13)}$$

Here only up to lth modes of vibration is considered. The ϕ_j is the jth mode shape of the link associated with jth mode of vibration δ_j. Two modes of link vibration are enough to completely represent the tip deflection. Now substituting equation (3.13) into equation (3.11), would result in

$$EI\phi'''' + \rho\phi\delta = 0 \text{ ..... (3.14)}$$

Separating the variables and equating to a constant, we get

$$\frac{EI}{\rho}\frac{\phi''''}{\phi} = -\frac{\ddot{\delta}}{\delta} = \omega^2 \text{ ..... (3.15)}$$

Now solving equation (3.15) will give the function for ϕ and δ as:

$$\delta_j = \exp\left(j\omega_j t\right) \text{ ..... (3.16)}$$

$$\phi_j(x) = C_{1,j}\sin(\beta_j x) + C_{2,j}\cos(\beta_j x) + C_{3,j}\sinh(\beta_j x) + C_{4,j}\cosh(\beta_j x) \text{ ....(3.17)}$$

The parameter ω_j in the equations (3.16) is jth natural angular frequency of the link undergoing deflection and β_j in the equation (3.17) is related to the natural frequency as $\beta_j^4 = \omega_j^2\rho/EI$. Applying the clamped boundary conditions to equation (3.13) will give

$$C_{3,j} = -C_{1,j} \quad \text{and} \quad C_{4,j} = -C_{2,j} \text{ ……..} \quad (3.18)$$

and with mass boundary conditions yield a 2X2 matrix equation

$$\begin{bmatrix} F_{1j} & F_{1j} \\ F_{2j} & F_{2j} \end{bmatrix} \begin{bmatrix} C_{1,j} \\ C_{2,j} \end{bmatrix} = \begin{bmatrix} 0 \\ 0 \end{bmatrix} \text{……} \quad (3.19)$$

Where $F_{11} = -\beta_j^2 \sin(\beta_j L) - \beta_j^2 \sinh(\beta_j L) - \frac{J_L}{\rho}\beta_j^5 \cos(\beta_j L) + \frac{J_L}{\rho}\beta_j^5 \cosh(\beta_j L)$

$$F_{12} = -\beta_j^2 \cos(\beta_j L) - \beta_j^2 \cosh(\beta_j L) + \frac{J_L}{\rho}\beta_j^5 \sin(\beta_j L) + \frac{J_L}{\rho}\beta_j^5 \sinh(\beta_j L)$$

$$F_{21} = -\beta_j^3 \cos(\beta_j L) - \beta_j^3 \cosh(\beta_j L) + \frac{M_L}{\rho}\beta_j^4 \sin(\beta_j L) - \frac{M_L}{\rho}\beta_j^4 \sinh(\beta_j L)$$

$$F_{22} = \beta_j^3 \sin(\beta_j L) - \beta_j^3 \sinh(\beta_j L) + \frac{M_L}{\rho}\beta_j^4 \cos(\beta_j L) - \frac{M_L}{\rho}\beta_j^4 \cosh(\beta_j L)$$

From equation (2.19), equating the det $|F|$ to zero will give a transcendental equation of function of β_j only while all other parameters are known in advance. Solving the equation $|F| = 0$, β_j for different modal frequencies can be determined. The transcendental equation resulting from equation (3.19) is given below as

$$\left(1 + \cos(\beta_j L)\cosh(\beta_j L)\right) - \frac{M_L \beta_j}{\rho}\left(\sin(\beta_j L)\cosh(\beta_j L) - \cos(\beta_j L)\sinh(\beta_j L)\right)$$
$$- \frac{J_L \beta_j^3}{\rho}\left(\sin(\beta_j L)\cosh(\beta_j L) + \cos(\beta_j L)\sinh(\beta_j L)\right) + \frac{M_L J_L \beta_j^4}{\rho^2}\left(1 - \cos(\beta_j L)\cosh(\beta_j L)\right) = 0$$

…… (3.20)

Now substituting the values of β_j in equation (3.19) constants can be calculated. The dynamical model can be derived Euler-Lagrange's equation given by equation (3.7) as

$$\begin{bmatrix} B'_{\theta\theta}(\theta,\delta) & B_{\theta\delta}(\theta,\delta) \\ B^T_{\theta\delta}(\theta,\delta) & B_{\delta\delta}(\theta,\delta) \end{bmatrix} \begin{bmatrix} \ddot{\theta} \\ \ddot{\delta} \end{bmatrix} + \begin{bmatrix} h_\theta(\theta,\delta,\dot{\theta},\dot{\delta}) \\ h_\delta(\theta,\delta,\dot{\theta},\dot{\delta}) \end{bmatrix} + \begin{bmatrix} 0 \\ K\delta + D\delta \end{bmatrix} = \begin{bmatrix} T_L \\ 0 \end{bmatrix} \quad \ldots\ldots\ldots\ldots \text{(3.21)}$$

Incorporating the actuator dynamics with flexible link dynamics the complete model can be obtained.

3.1.3. Finite element method model

In FE method the link is divided into finite number of elements separated from each other by nodes. Here the model of flexible link is derived using Lagrange's approach. First the modeling of each element is carried out and then they are combined satisfying some boundary conditions at nodes.

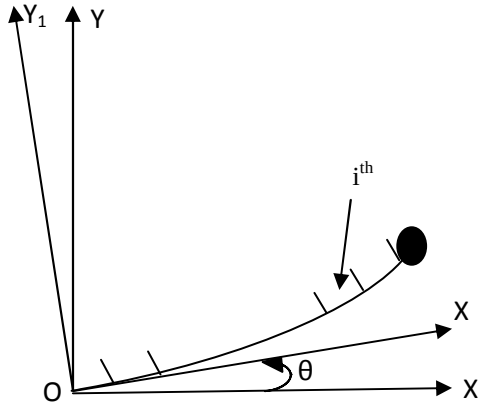

Fig. 3.3 Flexible link robot

The basic fundamental of FE method require the discretisation of the whole structure into a number of finite elements of standard structures. A node, the edge of the elements

where it is connected to the neighboring element is characterized by some coordinates called nodal coordinates. Any element can exhibit three different movements/motion at each nodes viz, longitudinal, transverse and rotational. However, in the case of beam which works under transverse loading so longitudinal motion is neglected. Therefore only transverse and rotational motion exists at nodes and is represented by $\left(v_1, \theta_1\right)$ and $\left(v_2, \theta_2\right)$ at nodes 1 and 2 respectively. The position of any point of i[th] element is given by

$$p(x,t) = x\theta + y_i(s,t) \quad \text{..... (3.22)}$$

where $y_i(s,t)$ is the deflection of the point of i[th] element while s is measured from the i[th] element. Thus we can write

$$x = (i-1)l + s \quad \text{..... (3.23)}$$

where l being the length of each element given by L/n, n being the number of elements of link. The dynamics of the flexible link is derived as follows:

- First the dynamics of each link is derived using Lagrange equation.
- Then models of each element are assembled with similar nodal coordinates at each node.
- Boundary condition is then imposed to get final model.

As already said the position of any point of the element is a function of transverse displacement and angular deflection of nodes. Therefore the position of any point in terms of nodal coordinates can be written as

$$y_i(s,t) = N_i Q_i = \sum_{j=1}^{4} \varphi_{i,j}(s) q_{i,2(i-1)+j}(t) \quad \text{..... (3.24)}$$

where N_i is called shape function of the element which denotes beam shape, Q_i is the nodal coordinate. By following the standard procedures the shape function is given by

$$N_i = \begin{bmatrix} 1-\frac{3s^2}{l^2}+\frac{2s^3}{l^3} \\ s-\frac{2s^2}{l}+\frac{s^3}{l^3} \\ \frac{3s^2}{l^2}-\frac{2s^3}{l^3} \\ -\frac{s^2}{l}+\frac{s^3}{l^2} \end{bmatrix}^T \quad \text{..... (3.25)}$$

and the associated nodal varibles

$$Q_i = \begin{bmatrix} q_{i,2(i-1)+1} \\ q_{i,2(i-1)+2} \\ q_{i,2(i-1)+3} \\ q_{i,2(i-1)+4} \end{bmatrix} \quad \text{..... (3.26)}$$

The equation (3.22) now can be written as

$$p(x,t) = x\theta + N_i Q_i = \begin{bmatrix} x & \varphi_{i,1} & \varphi_{i,2} & \varphi_{i,3} & \varphi_{i,4} \end{bmatrix} \begin{bmatrix} \theta \\ q_{i,2(i-1)+1} \\ q_{i,2(i-1)+2} \\ q_{i,2(i-1)+3} \\ q_{i,2(i-1)+4} \end{bmatrix} \quad \text{..... (3.27)}$$

Here we will derive the dynamical model of ith element using Lagrange approach, i.e. finding out the KE and PE associated with the ith element of the flexible link and then satisfying the Lagrangian which is the difference of KE and PE of the element Euler-Lagrange equation given by equation (3.7). The KE of the ith element is given by

$$T_i = \frac{1}{2}\int_0^l \rho\left(\frac{\partial p(s,t)}{\partial t}\right)^2 ds \quad \text{..... (3.28)}$$

Using equation (3.27) the KE can be written as

$$T_i = \frac{1}{2}\dot{Q}_a^T M \dot{Q}_a \quad \text{..... (3.29)}$$

Where M is the inertia matrix and Q_a is the nodal variables and is given by

$$M = \int_0^l \rho N_a^T N_a ds$$

Where $$N_a^T N_a = \begin{bmatrix} x \\ \varphi_{i,1} \\ \varphi_{i,2} \\ \varphi_{i,3} \\ \varphi_{i,4} \end{bmatrix} \begin{bmatrix} x & \varphi_{i,1} & \varphi_{i,2} & \varphi_{i,3} & \varphi_{i,4} \end{bmatrix} \text{..... (3.30)}$$

and $$Q_a = \begin{bmatrix} \theta & q_{i,2(i-1)+1} & q_{i,2(i-1)+2} & q_{i,2(i-1)+3} & q_{i,2(i-1)+4} \end{bmatrix}^T \text{..... (3.31)}$$

Similarly the PE of the ith element is given by

$$U_i = \frac{1}{2}\int_0^l EI\left(\frac{\partial^2 p(s,t)}{\partial s^2}\right)^2 ds \quad \text{..... (3.32)}$$

This can be simplified as $U_i = \frac{1}{2} Q_a^T K Q_a$

Where K is the stiffness matrix and is given by

$$K = \int_0^l EIK_a^T K_a ds \text{ and } K_a = \frac{\partial^2 N_a}{\partial s^2}$$

Using equation (3.30) the inertia matrix and stiffness matrix can be derived. It is to be noted here that both matrix corresponds to the ith element of the link and are of having constant entries with symmetric property. Thus the matrix can be given as

$$M = \frac{\rho l}{420} \begin{bmatrix} m_{11} & m_{12} & m_{13} & m_{14} & m_{15} \\ m_{12} & 156 & 22l & 54 & -13l \\ m_{13} & 22l & 4l^2 & 13l & -3l^2 \\ m_{14} & 54 & 13l & 156 & -22l \\ m_{15} & -13l & -3l^2 & -22l & 4l^2 \end{bmatrix} \quad \ldots\ldots\ldots\ldots\ldots\ldots\ldots \quad (3.33)$$

$$K = \frac{EI}{l^3} \begin{bmatrix} 0 & 0 & 0 & 0 & 0 \\ 0 & 12 & 6l & -12 & 6l \\ 0 & 6l & 4l^2 & -6l & 2l^2 \\ 0 & -12 & -6l & 12 & -6l \\ 0 & 6l & 2l^2 & -6l & 4l^2 \end{bmatrix} \quad \ldots\ldots\ldots\ldots\ldots\ldots\ldots\ldots\ldots\ldots\ldots \quad (3.34)$$

where the elements of inertia matrix are

$$m_{11} = 140l^2 \left(3i^2 - 3i + 1\right)$$

$$m_{12} = 21l \left(10i - 7\right)$$

$$m_{13} = 7l^2(5i-3)$$

$$m_{14} = 21l(10i-3)$$

$$m_{15} = -7l^2(5i-2)$$

Once the energies associated with i[th] element is find out, then it is repeated for all n elements of the link. The KE and PE of the link can now be obtained as summing up all the respective energies of the all the elements. Since the inertia and stiffness matrices are of order 5×5 for single element the order of these matrices for whole link (n elements) as a whole would be $5+2(n-1)\times5+2(n-1)$. However the link under consideration is of cantilever beam with one end fixed results in no movement at fixed end. So incorporating the boundary conditions the order of the matrices would reduces to $3+2(n-1)\times3+2(n-1)$. The KE and PE of the whole link can be mathematically represented as

$$T = \sum_{i=1}^{n} T_i \quad \text{and} \quad U = \sum_{i=1}^{n} U_i \qquad \ldots\ldots\ldots\ldots\ldots\ldots\ldots\ldots \quad (3.35)$$

Exploiting equations (3.29), (3.32), (3.35) into equation (3.7) the dynamical model of the flexible link would result. The dynamical model of the link in compact form can be written as

$$M\ddot{Q} + KQ = T \qquad \ldots\ldots\ldots\ldots\ldots\ldots\ldots\ldots\ldots\ldots \quad (3.36)$$

This equation represents dynamical model of the flexible link without any damping term. Passive damping can be included into equation (3.36) based on Rayleigh's proportional damping which is given by

$$C = \alpha M + \beta K \quad \text{..... (3.37)}$$

Thus the dynamics of the flexible link can be modified as

$$M\ddot{Q} + C\dot{Q} + KQ = T_L \quad \text{..... (3.38)}$$

Equation (3.38) along with equation (3.6) completely describes the dynamics of flexible link.

3.2. State space representation of the dynamics of flexible link

State space representation of the model is necessary for design and analysis of the controller. So before we focus on the controller state space model is obtained. Here the model of the link has been derived separately for actuator, link and given in equations (3.1), (3.6), (3.21) and (3.38). In this work the dc motor dynamics separately incorporated for ease in understanding the operation of flexible link in practical aspects. However the inclusion of motor dynamics increases the order of state space by one. Referring equations (3.1), (3.6) and (3.21) the state space representation of the AMM model can be written as

$$\left.\begin{aligned} \dot{X} &= AX + Bu \\ Y &= CX + Du \end{aligned}\right\} \quad \text{..... (3.39)}$$

where $X = \begin{bmatrix} \theta_L & \delta & \dot{\theta}_L & \dot{\delta} & i_a \end{bmatrix}^T$

$$A = \begin{bmatrix} 0_{2\times2} & I_{2\times2} & 0 \\ -B^{-1}K & -B^{-1}(h'+D) & B^{-1}P \\ 0_{1\times2} & S & -\dfrac{R_a}{L_a} \end{bmatrix}, \quad B = \begin{bmatrix} 0_{2\times1} \\ 0_{2\times1} \\ \dfrac{1}{L_a} \end{bmatrix}$$

$$C = \begin{bmatrix} I_{5\times5} \end{bmatrix}, \qquad D = \begin{bmatrix} 0_{5\times5} \end{bmatrix},$$

and $K = \begin{bmatrix} 0 & K_\delta \end{bmatrix}^T$, $D = \begin{bmatrix} 0 & D_\delta \end{bmatrix}^T$, $P = \begin{bmatrix} N_r K_t & 0 \end{bmatrix}^T$, $S = \begin{bmatrix} -\dfrac{N_r K_t}{L_a} & 0 \end{bmatrix}$

Similarly the state space representation of the FEM model is given in equation (3.40). The state vectors here are different from AMM model and the order of the system matrix depends on number of elements being considered in analysis than how many modes are taken into consideration in assumed mode method.

$$X = \begin{bmatrix} Q & \dot{Q} & i_a \end{bmatrix}^T$$

and $$A = \begin{bmatrix} 0 & I & 0 \\ -M^{-1}K & -M^{-1}C & M^{-1}RN_rK_t \\ 0 & S & -\dfrac{R_a}{L_a} \end{bmatrix}, \; B = \begin{bmatrix} 0 \\ 0 \\ \dfrac{1}{L_a} \end{bmatrix}$$

$$C = \begin{bmatrix} I_{3+2(n-1)\times3+2(n-1)} \end{bmatrix}, \quad D = \begin{bmatrix} 0_{3+2(n-1)\times3+2(n-1)} \end{bmatrix}, \; R = \begin{bmatrix} 1 \\ 0_{2+2(n-1)\times1} \end{bmatrix}$$

3.3. Experimental setup of flexible robot system

Quanser two DOF serial flexible link robot consists of two serial flexible links manufactured by Quanser. It is primarily designed for laboratory experimental work for the students, researchers to carry out the real time analysis of the studies and let them understand real world industry problems. In the control & robotics lab of NIT Rourkela two link flexible robot developed by Quanser [26] is available for study of control objective of flexible robot. It consists of two serial flexible links actuated by dc motor instrumented with strain gauges for tip deflection measurement. The main components of the setup are the linear amplifier, Q8 terminal board, DAQ system and different sensors like strain gauge, quadrature optical encoder, limit switches. These are discussed in detail in subsequent sections.

3.3.1. Flexible links

The robot is provided with two flexible links of different dimensions. Both these link is made of wear resistant 1095 spring steel. This steel is capable of Rockwell C55 hardness at low tempering temperatures. Both links are of same length but with different width and thickness and their dimension is given in the table 3.1.

TABLE 3.1 FLEXIBLE LINK PARAMETERS

Parameters	Length in cm	Width in cm	Thickness in cm
Link 1	22	7.62	2.261
Link 2	22	3.81	0.127

The links are mounted to the actuator through the speed reducer. At the base of the links strain gauge is fabricated for tip deflection measurement.

3.3.2. Sensors

There are different sensors used for different measurement of signals like optical encoder for angular position measurement, strain gauge for strain measurement, limit switches for limiting maximum and minimum positions etc. The details of the sensors are discussed below.

Strain gauge: Strain gauge consists of a thin metallic elastic material as a strain measurement and it is mounted on the place where the body is subjected to strain. The basic principle of operation is that the strain on the body causes strain gauge to undergo some changes in the length and this length is calibrated in terms of measurement of interest. Normally a balanced bridge circuit (Wheatstone bridge) is used with strain gauge forming one of its arms. Any change in length of the gauge changes the resistance and hence voltage leading to bridge unbalanced. The relationship between dimension of the body and resistance is given by

$$R = \eta \frac{l}{a} \quad \text{..... (3.40)}$$

where l, a and η are the length, area of cross-section of the body and resistivity of the body. The voltage generated is given in terms strain created by the body in mm/mm. Here the tip deflection is measured by the gauge which is mounted at the base. The movement of the tip in either direction creates strain at the base, i.e. length of the gauge

increases so resistance and voltage. This strain is calibrated in terms of deflection in meter [26] and is given by

$$y = \frac{2}{3}\frac{E_b L_b^2}{T} \quad \text{..... (3.41)}$$

The L_b is the length of the link measured up to strain gauge from free end, T is the thickness of the link, $E_b = 6FL_b \big/ YXT^2$ is strain in mm/mm at the base, Y is young's modulus of elasticity, F is load force at the tip in N, X is the width of the flexible link.

The strain gauge measurement circuitry is provided at the base for operation of the bridge circuit. It consists of two potentiometers each having 20 turns, viz, gain potentiometer and offset potentiometer. The former supplies power to the bridge while the later is used for zero tuning of the circuit to remove any offset voltage that might have kept. The gain potentiometer has a constant gain of 2000 while gain of offset potentiometer is adjusted for zero measurement under no loading at the tip.

Q-Optical encoder: Quadrature optical encoder is used for angular position measurement very precisely. It consists of two inputs, viz. channel A and channel B which is placed 90 degree apart from each other. Besides these a third input called *index* input exists which provides single pulse per revolution for precise measurement of reference position. The position of these inputs of optical encoder is shown below. The optical encoder is mounted on the shaft of the motor and on the periphery of the disc two digitally encoded signals is placed over it. A photo sensor and light emitting diode is placed on opposite side of the disc.

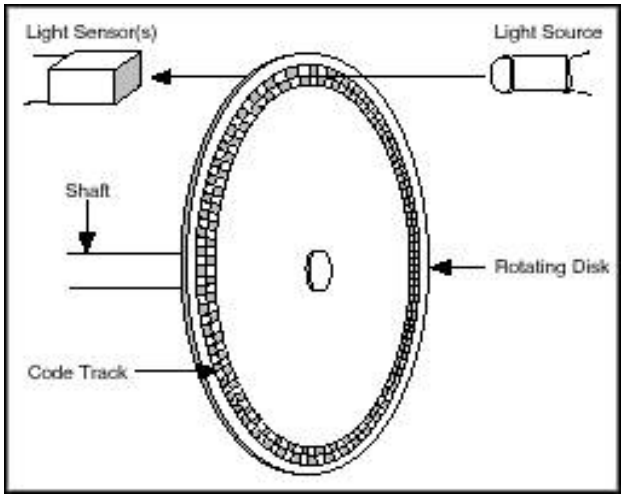

Fig. 3.4 Operation of optical encoder

When light is detected by the sensor it is encoded as one (1) otherwise zero (0). At any time only two inputs are encoded based on whether the photo sensor is activated or not. The two encoded signal on the disc is represented by digital pulses.

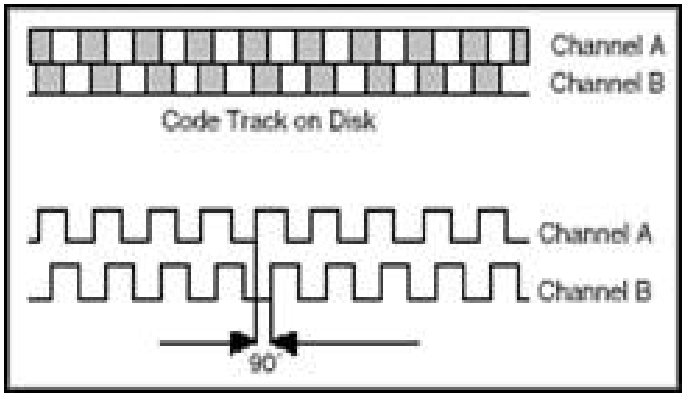

Fig. 3.5 Quadrature operation of optical encoder

When the motor rotates signals are encoded as digital pulses and a cycle is counted when there four transitions of digital pulses occur (00, 01, 10, 11). So if counter counts 1024 lines per revolution of the encoder it actually has 1024X4=4096 counts/rev. Therefore we can say the optical encoder is of resolution 4 times the counts of the encoder. Here it

counts 1024 lines/rev so it will have 4096 counts/rev. The angular position counted per revolution of the encoder is $(360/4096)(\pi/180) = 0.0015$ rad/rev.

Limit switches: There are two limit switches for each link mounted at maximum and minimum positions of rotation of flexible link robot. These sensors are used to ensure the safe operation of mechanical unit. These are basically hall effect sensors with three terminals device manufactured by Hamlin. It requires ± 15 VDC supply for its operation.

3.3.3. Actuators

In robotics application dc motors are widely used as actuators because of ease in control. However pneumatic type actuators can also be used in some specific applications. The dc motor rotates at very high speed which is reduced to some safe value by speed reducer. Here harmonic drive is used for speed reduction and is placed coaxial with the actuator. Harmonic drives possess many advantages over conventional gear train box in terms zero backlash, not bulky, lightweight and precise high gear ratio. Link 1 is coupled with the maxon 273759 precision brush motor of 90 watts and link 2 is coupled with maxon 118752 precision brush motor of 20 watts. Both optical encoder and harmonic drives are mounted on the motor shaft. The harmonic drives are manufactured by Harmonic drive LLC.

The basic principle of operation of harmonic drive is based on a strain wave gearing theory. The constructional features consist of an outer circular spline, flex spline and wave generator. The wave generator is fixed to the motor shaft and it has an elliptical disk with outer ball bearing provision. The circular spline is a rigid fixed circular cylinder

with teeth present along the inner surface. The flex spline is a flexible thin structure which deforms to the shape of circular spline. The arrangements of these three parts are given in figure. Both wave generator and flex spline are placed inside the circular spline such that the tooth of the flex spline exactly fits with teeth of circular spline as the rotation starts along the major axis of wave generator.

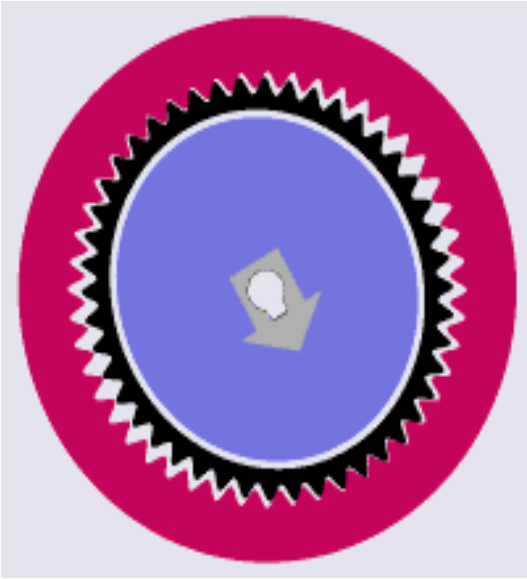

Fig. 3.6 Harmonic Drive

The dc motors are manufactured by Maxon swiss and the ratings are given in table 3.2. The mechanical parameters of hub 1 are given in table 3.3.

TABLE 3.2 ACTUATOR SPECIFICATIONS

Motor specification	**Link 1**	**Link 2**
Armature resistance	11.5 Ω	2.32 Ω
Armature inductance	3.16 mH	0.24 mH
Torque constant	0.119 Nm/A	0.0234 Nm/A
Back emf constant	0.119 Vs/rad	0.0234 Vs/rad

TABLE 3.3 FLEXIBLE LINK SYSTEM PARAMETERS

Parameters	Link 1	Link 2
Maximum continuous current	0.944 A	1.21 A
Gear ratio	100	50
Moment of inertia at motor shaft	$6.28X10^{-6}$ Kg m^2	$1.03\ X10^{-6}$ Kg m^2
Moment of inertia of drive mounting bracket	$7.361X10^{-4}$ Kg m^2	$444.55X10^{-6}$ Kg m^2
Moment of inertia of compounded end effector system	0.17043 Kg m^2	0.0064387 Kg m^2
Torsional stiffness constant	22 Nm/rad	2.5 Nm/rad
Mechanical time constant	5 ms	4 ms
Young's modulus of elasticity	$2.0684X10^{11}$ Pa	$2.0684X10^{11}$ Pa

3.3.4 Linear current amplifier

A linear current amplifier with two channels is provided by Quanser. The two motors are actuated by control signal from this amplifier. It provision for current measurement, to enable/disable it.

TABLE 3.4 AMPLIFIER SPECIFICATIONS

Parameters	Each Channel
Maximum continuous current	3 A
Peak current	5 A
Maximum continuous voltage	28 V
Peak power	300 W
Bandwidth	10 KHz
Gain	0.5 A/V

The control signal from Q8 terminal board to the motor goes through amplifier. The amplifier provides a constant current to voltage gain of 2V/A. The specification of the linear current amplifier is given in table 3.4.

3.3.5 Cables

There are different types of cables are used for different purposes like analog, digital, encoder etc. These cables perform their respective function. The details about these cables are discussed below.

Motor Cables: These cables carry signals from amplifier to motor. It consists of four leads two for dc motors, one for ground and other one is left unconnected.

Fig. 3.7 Motor Cables

Encoder Cables: Optical encoder generates encoded signal which is transmitted by encoder cables to the Q8 terminal board which is required for the design of the controller.

Fig. 3.8 Encoder Cables

Analog Cables: Signals like from strain gauge, current sensor are of analog type and the signals before their use they must be converted into digital. So these analog cables carry signals to Q8 terminal board for their conditioning.

Fig. 3.9 Analog Cables

Digital Cables: Digital I/O cables are used for communication with PC which handles digital signals. Sometimes some components need to be enabled and/or disabled in some specific operation of the manipulator and digital signal shows better flexibility.

Fig. 3.10 Digital I/O Cables

3.3.6 External power supply

There is provision for external power supply at ±15 VDC. There are some sensors like strain gauge, limit switches require the dc power for their operation. It consists of an adapter along with power cable.

Fig. 3.11 External Power Supply

3.3.7 Q8 terminal board

It is an interfacing terminal board for signals coming from different parts with the PC. In fact, it forms the platform where a different control signals communicate with the plant and user. This board has provisions for analog I/O, digital I/O, encoder signals etc. The different signals must be converted into digital before they are used in the control algorithm. Here core2duo processor implements the control algorithm. Quanser hardware-in-loop (HIL) board conditions different signals and sends digital signals to the processor. The communication between Q8 terminal board and processor is performed by 32 bit digital I/O ports. The Q8 terminal board is shown in Fig.3.12. Besides this, it also provides enable signals to amplifier and to choose different channels as well. In Fig.3.12 it is shown that it has eight analog and analog outputs, eight encoder ports, four digital input and output ports, ports to communicate with controller. MATLAB has provisions to support files to integrate with Quanser driver files so that the models will run in real time. The control signals generated by controller is digital but the motor requires analog signals. The HIL board performs the digital-to-analog conversion (DAC) and sends it to the motor.

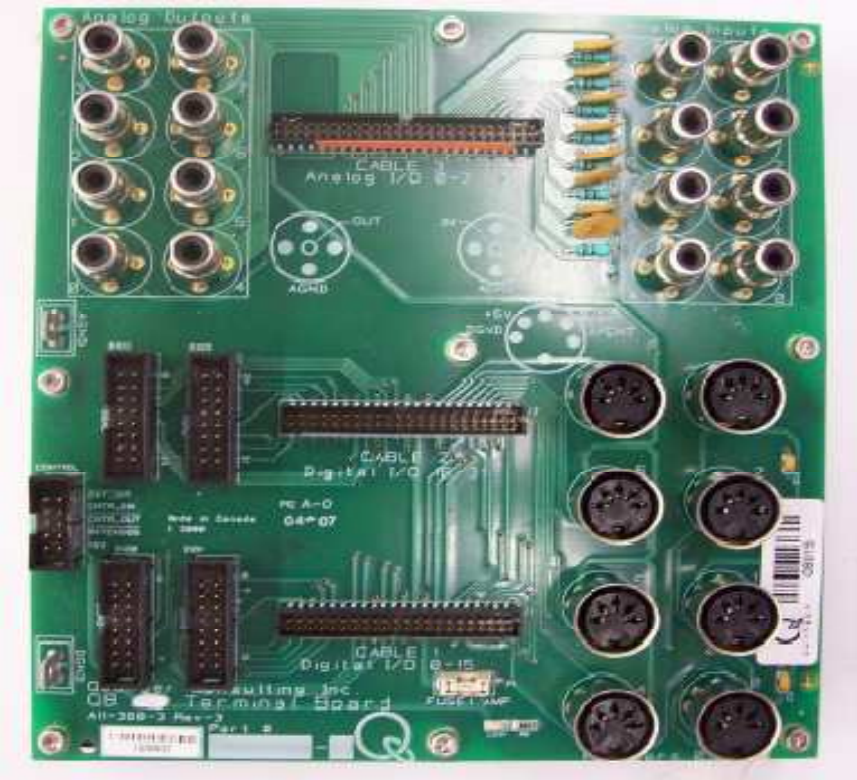

Fig. 3.12 Q8 Terminal board

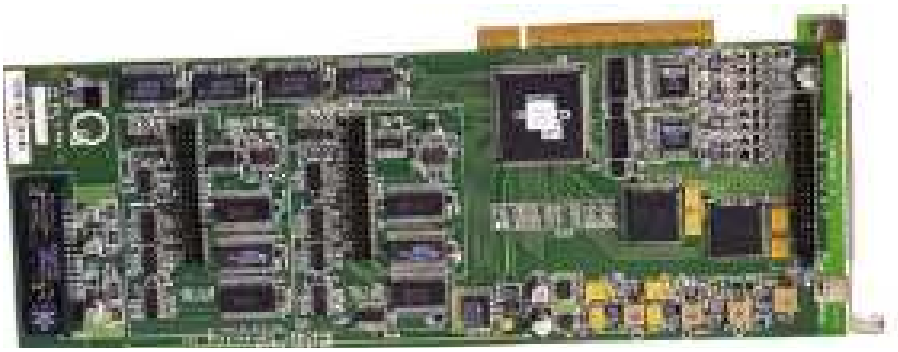

Fig. 3.13 Hardware-In-Loop (HIL) board

The Q8 board takes 17.8 μsec with all eight channels working simultaneously for analog-to-digital conversion (ADC) and for DAC it takes 1.35 μsec. It is to be noted here that only four analog input channels and two analog output channels are being used so that the time requirement for ADC and DAC conversion is reduced. The real time model execution depends on these data conversion rates.

3.4 Interfacing with MATLAB/SIMULINK

The control algorithm is implemented on core2duo processor through MATLAB/SIMULINK. The flexible link robot is interfaced with MATLAB software. The interface between flexible link robot and MATLAB is done by the QuaRC software which allows the SIMULINK models to run in real-time target seamlessly. The software allows the users to build the model and then connect it to target before running it.

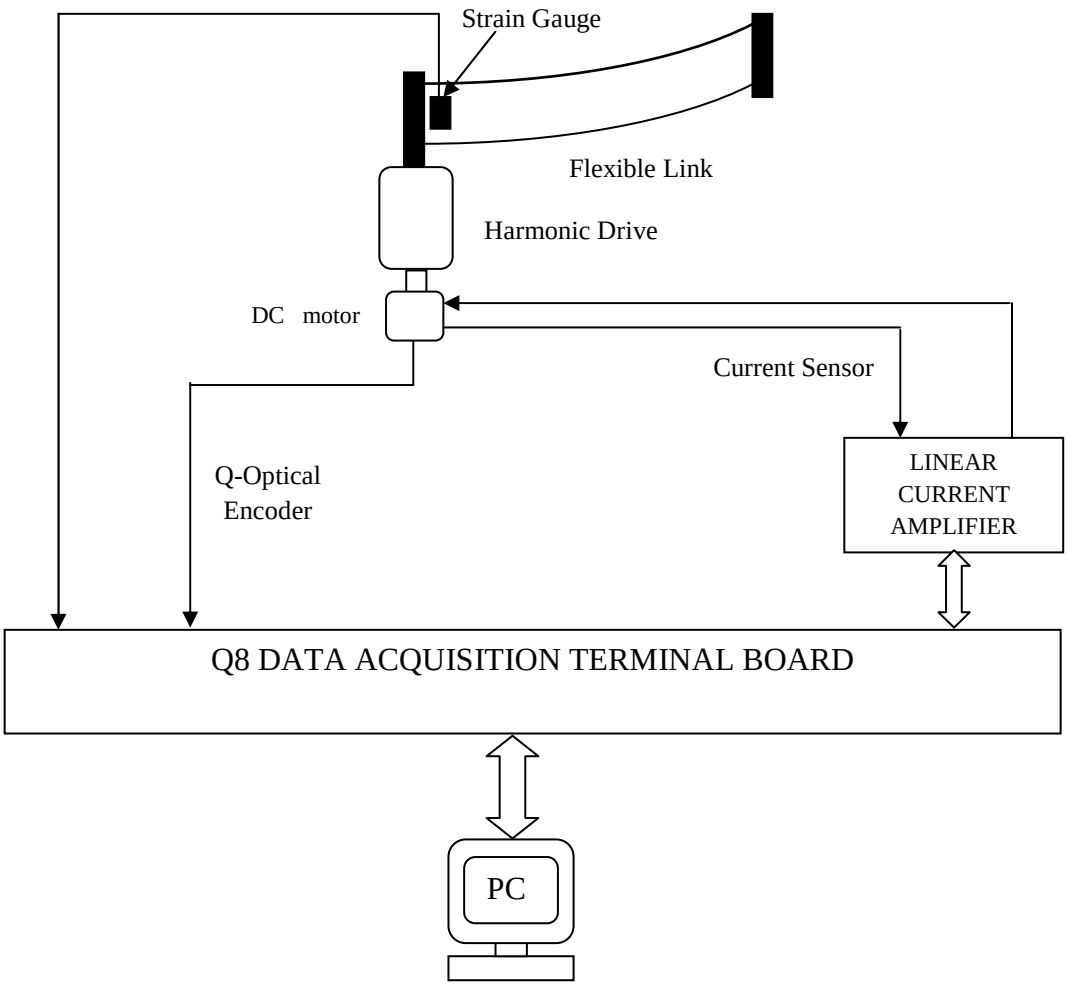

Fig. 3.14 Quanser Single Link Flexible Robot System

The experimental block diagram of flexible link manipulator is shown in Fig.3.14. User communicates with real-time set up through iBall PC on Windows XP platform. The controller developed by user is implemented using MATLAB/SIMULINK which is integrated with the real time plant by QuaRC software. The results of experiments are obtained in SIMULINK environment.

3.5 Experimental validation of the model

The model derived using assumed mode method and finite element methods are validated with experimental results in open loop condition. In both the cases, a bang-bang torque input with 0.5 Nm for 0.3 sec and -0.5 Nm for 0.3 sec to 0.6 sec is given to both real time plant and mathematical models. The bang-bang input is shown in Fig.3.15. The experimental results are compared with simulation results for both AMM and FEM models and are shown in Fig.3.16 and Fig.3.17.

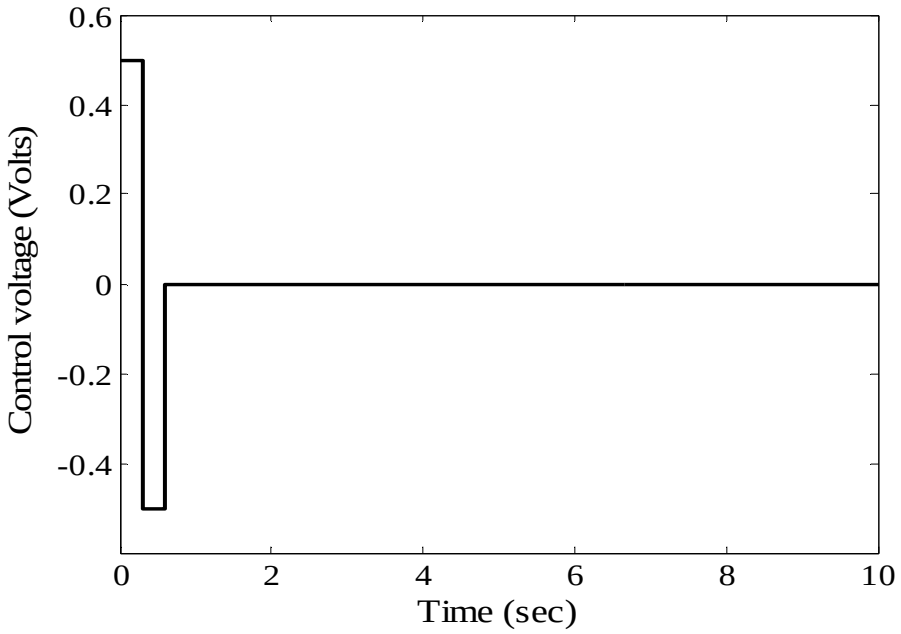

Fig. 3.15 Bang-bang input

3.5.1 Results of assumed mode method model

The response of flexible link robot to bang-bang input is analyzed both by simulation and experimental studies. The hub angle, tip deflection and tip trajectory of both assumed mode model and real time plant are compared. The results of hub angle, tip deflection and tip position are shown in Fig. 3.16 (a)-(c) respectively. It shows that simulation results agree with that of experimental results. During negative excursion the experimental result of hub angle decreases after some time than that of simulation result in Fig.3.16 (a). This is due to at 0.3 sec the response of tip to negative torque gives a delayed response so is the hub angle. The frequency of vibration of assumed mode model is also consistent with experimental results as shown in Fig.3.16 (b).

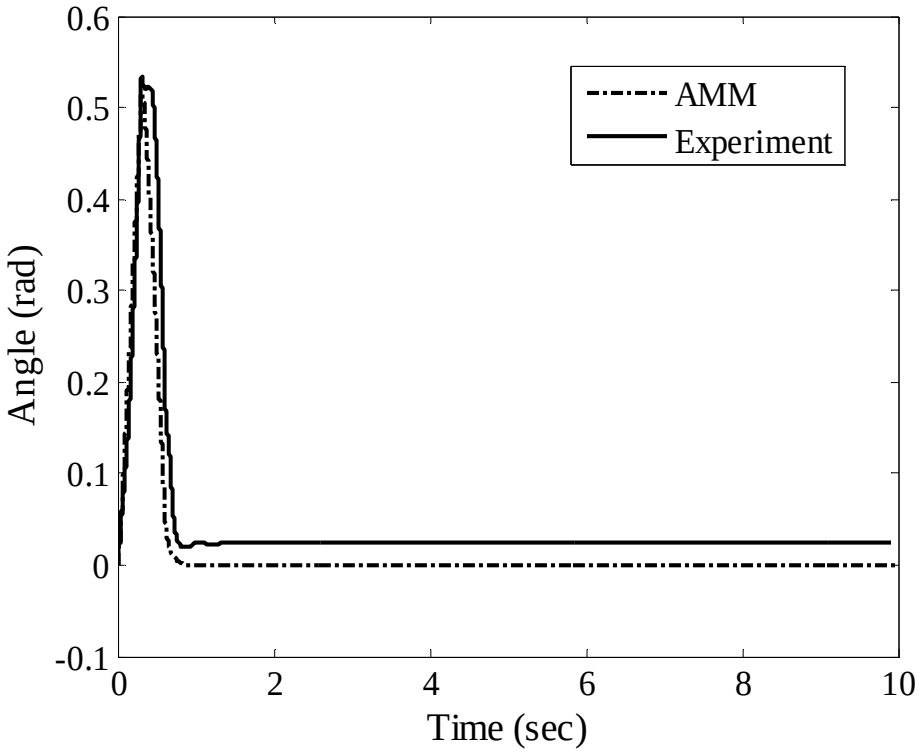

Fig. 3.16 (a)

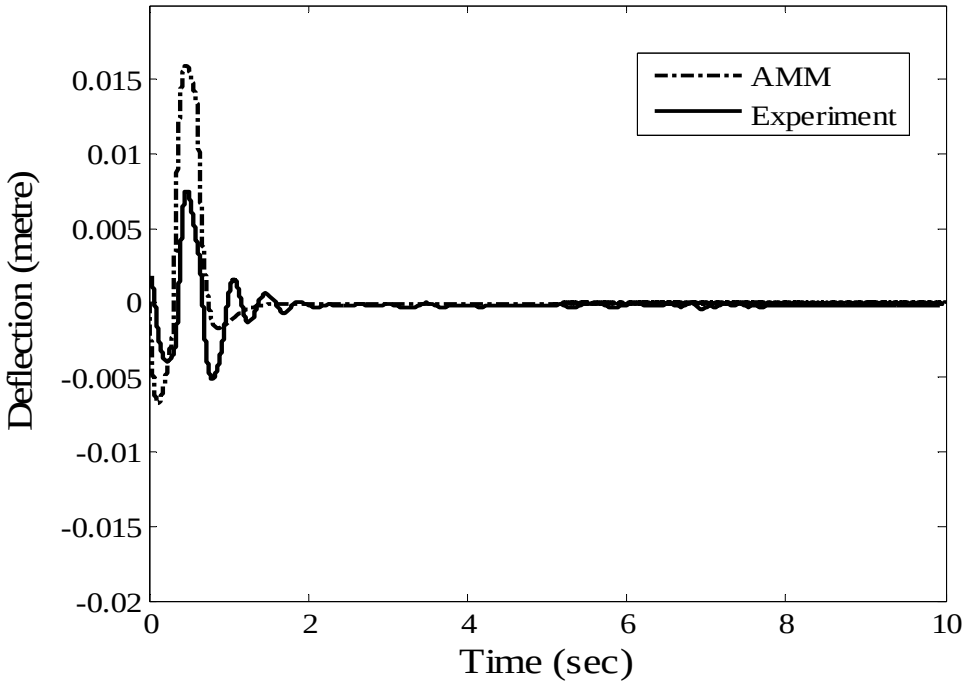

Fig. 3.16 (b)

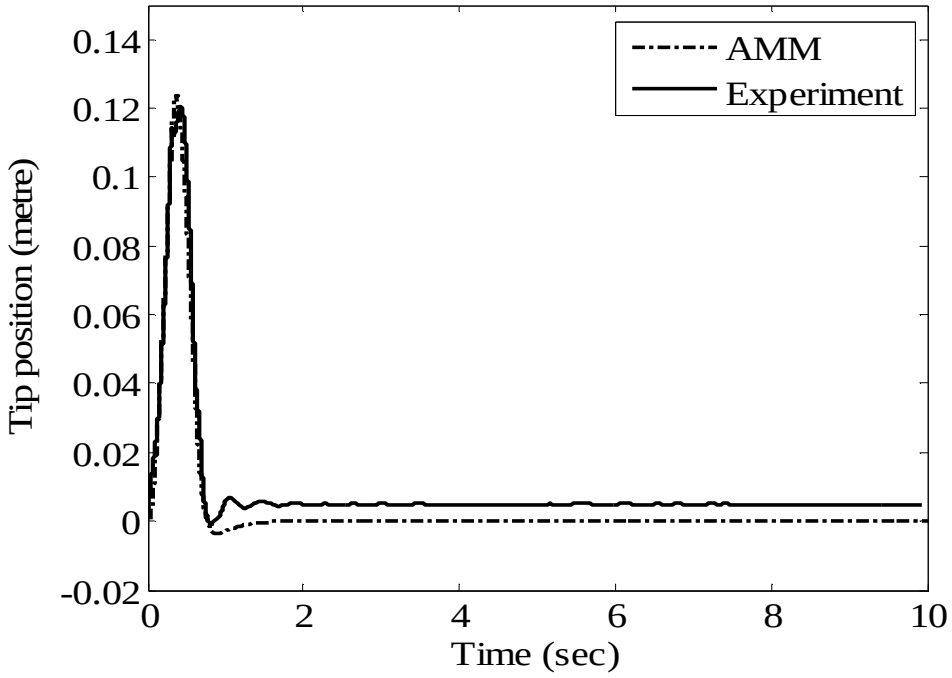

Fig. 3.16 (c)

Fig. 3.16 AMM model validation results with bang-bang input (a) Hub angle, (b) Tip deflection and (c) Tip trajectory

3.5.2 Results of finite element method model

The experimental study of finite element model is also analyzed for same bang-bang input voltage. The results obtained from finite element model are compared with experimental results. Here, only one element is considered in deriving the model because single element can result in more than 87% accuracy [10]. The tip deflection, tip trajectory and hub position of simulation and experimental results are plotted in Fig.3.17 (a)-(c) respectively. Hub angle of both AMM and FEM model differ slightly because of non-minimum phase characteristic of tip which is not compensated in the deriving the model. However, in the controller design necessary care can be taken for non-minimum phase characteristics. The tip trajectory responses of AMM model agree quite closely with that of experimental results (Fig.3.17).

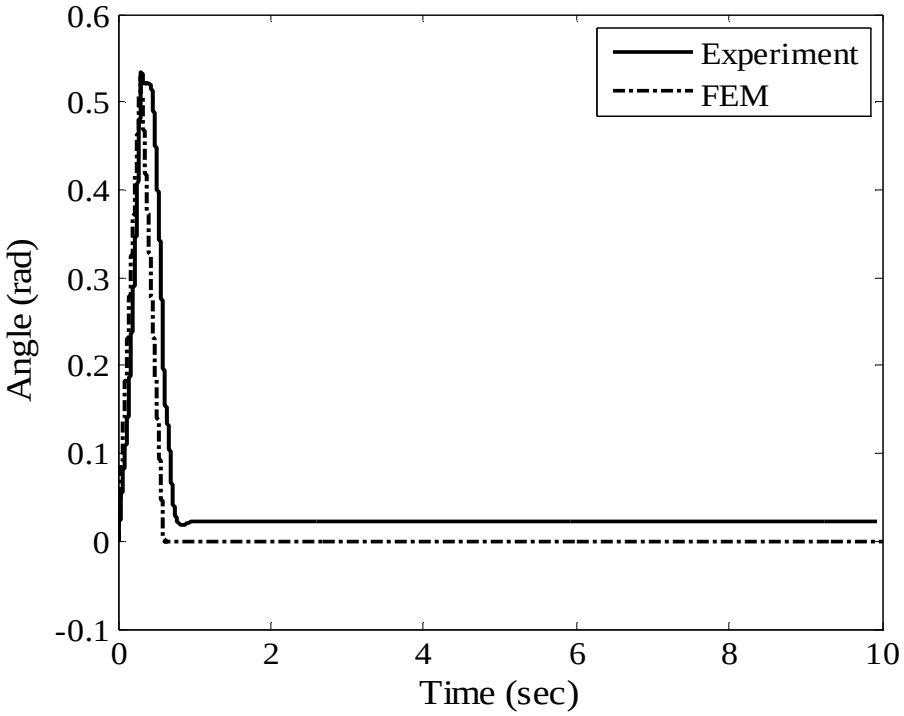

Fig. 3.17 (a)

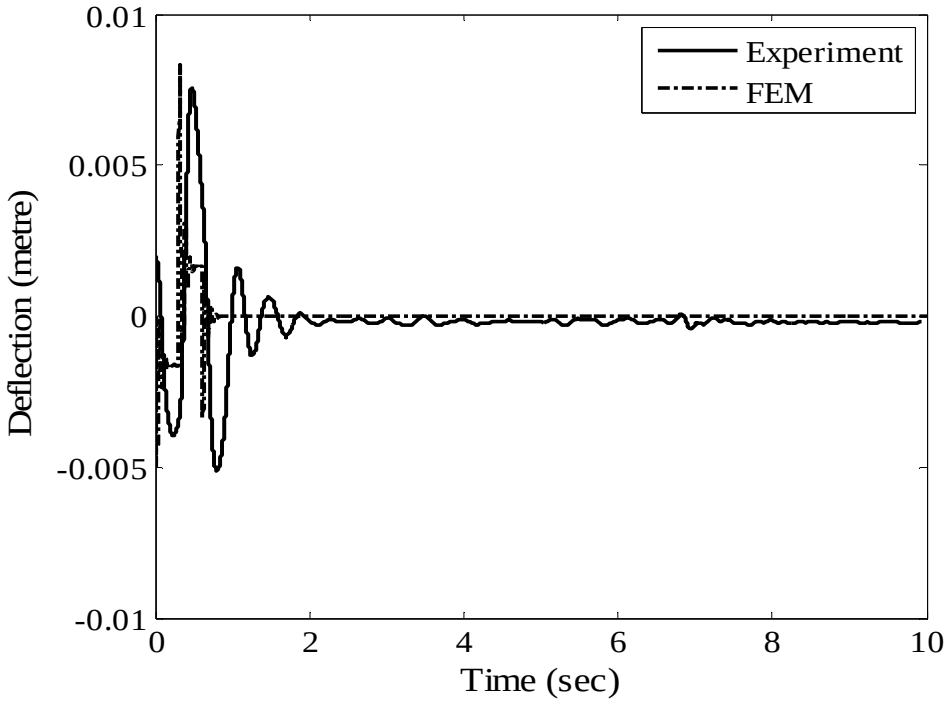

Fig. 3.17 (b)

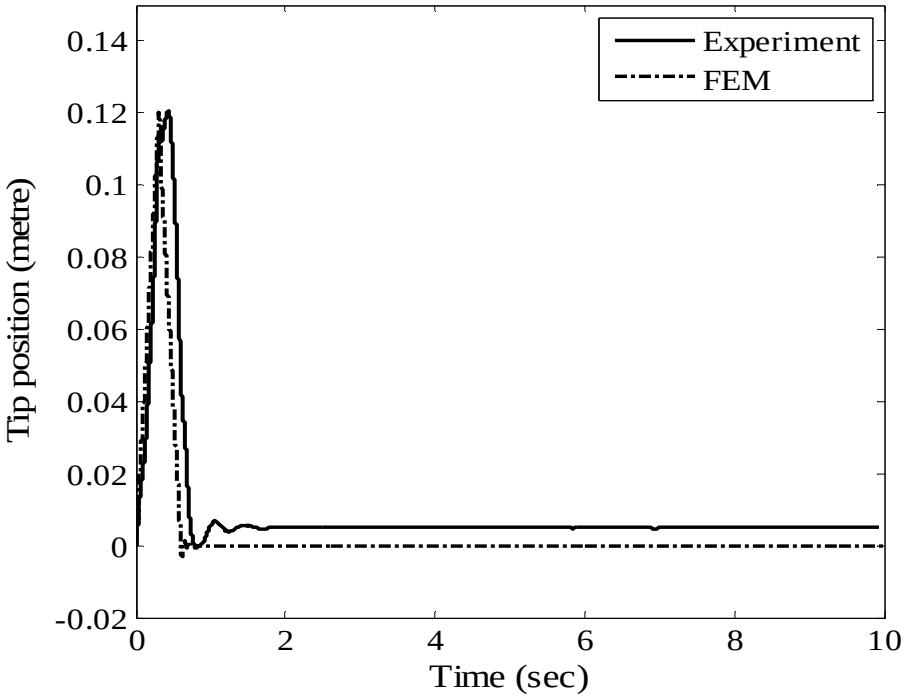

Fig. 3.17 (c)

Fig. 3.17 FEM model validation results with bang-bang input (a) Hub angle, (b) Tip deflection and (c) Tip trajectory

3.6 Summary

Modeling of actuator (dc motor) is done in section 3.1.1 separately and then flexible link dynamics is derived using assumed mode and finite element method in subsequent sections. In finite element method only one element is considered to derive the model. Then experimental test bed is briefly discussed in section 3.3 followed by real time integration with MATLAB/SIMULINK. The open loop model validations are reported in section 3.5 by providing the bang-bang input to the dc motor with amplitude of 0.5 for 0.3 sec only. It is shown that both simulation and experimental results agree with each other.

Chapter 4

Tip Position Controller for Flexible Link Robot

4.1 Introduction

The different control techniques have been developed for single/multilink flexible robots. The flexible link robot is a single link multi output (SIMO) system with input and outputs are non-collocated in which the input to the system is less than the input. Initial works used linear control techniques based on the transfer function model of the robot. Some earlier works of Canon and Schimtz [28], Oakley and Canon [29] derived non linear model using assumed mode description and PD controller was designed from linearised model. They carried out both simulation and experimental work for their designed PD controller to a step command. The transfer function model reveals that presence of right-half s-plane zero which is characterized by delayed response. However, over the last two decades due to development in control area many controllers have been developed for flexible link robot. Some of the noted work of A De Luca and Siciliano [15] addressed inversion control of assumed mode method model, optimal control for single link by Canon and Schimtz [28], inner and outer stabilizing loop control by H Geniele *et al* [14] are worth to be noted. In recent years some of the nonlinear control

techniques have been designed and promising aspects of soft computing approaches have motivated researchers to use it for flexible link robot.

In this chapter the concentration is made towards the end point control of flexible link robot. Since the manipulator is required to move to the final position with minimum/zero vibration of tip and we expect simple controller such as PD would be enough for controlling the tip vibration. The next section discusses such controller for regulation problem of flexible link robot.

4.2 Tip feedback controller

The tip feedback controller as its name suggests, tip deflection is fed back into the controller for vibration control of flexible structure. PD controller is very effective even for some complex systems given the gains are properly chosen. The gains play an important role in the performance of PD control however unavailable of many standard procedures for choosing optimum gains often limit its application to wide class of systems. Notwithstanding PD control is widely used in different systems with satisfactory results motivating many researchers to incorporate different intelligent tools for gain optimization. Here the tip feedback controller is devised by feeding tip deflection to PD controller as

$$u = -K_p\left(\theta(t) - \theta_{des}\right) - K_d\dot{\theta}(t) - K_f\dot{y}(L,t) \quad \text{..... (4.1)}$$

where $\theta(t)$ is the hub angle of the link.

θ_{des} is the constant final position.

$\dot{\theta}(t)$ is the angular velocity of the obtained by derivative filter.

$\dot{y}$ is the rate of change of tip deflection measured by strain gauge and derivative filter.

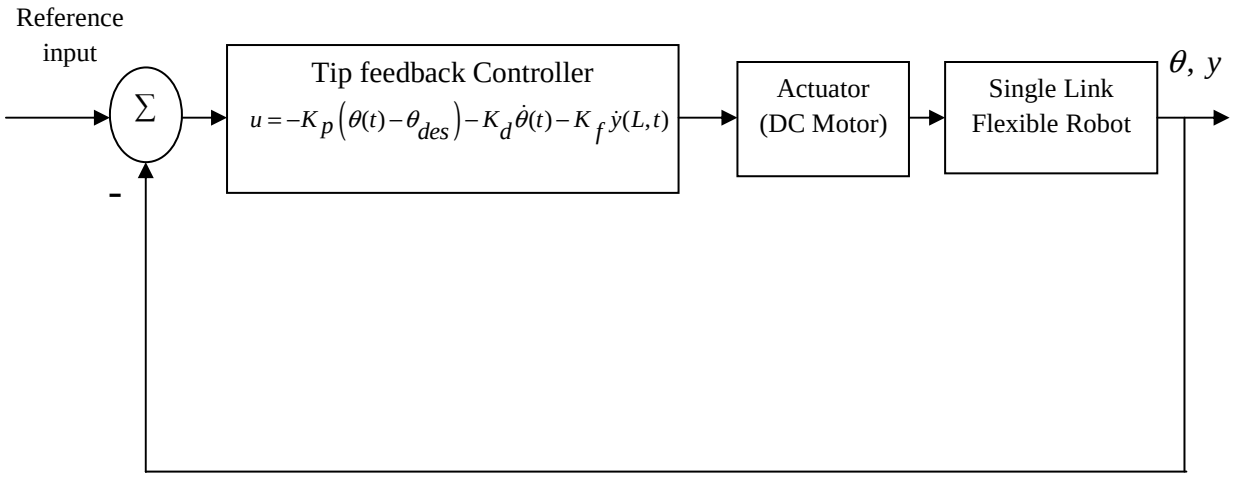

Fig. 4.1 Block diagram of tip feedback controller

The block diagram representation of system with controller is shown in Fig.4.1. Here our reference input is a constant position because of regulation problem. The controller drives the motor but in practical case there is amplifier of some gain which drives the motor. The flexible is instrumented with sensors for measurements of different signals such as hub angle and tip deflection. In our controller we need the rate of change of these measurements, so derivative filters are used in practice. Optical encoder and strain gauge provides the hub angle and tip deflection measurements. These signals are fed back to the input where the error signal is calculated. This error and rate of error signal are directly used in our controller which drives the flexible robot and closed loop operation of system is achieved.

The controller structure is very simple with first term is proportional and second term indicates derivative controller. It is noted that rate of tip deflection is incorporated into the PD controller to effectively suppress the vibration of flexible robot. The structure of the controller with relevant to practical implementation is shown in Fig.4.2. Strain gauge measure tip deflection in meter as per equation (3.41) and optical encoder provides the joint variables. These sensor signals are directly used in the controller design. The gains K_p, K_d and K_f are constants exclusively determine the performance of the proposed controller. At this point it can be said that any arbitrary chosen gains might not result better tip performance even may lead to system unstable. Hence tradeoff gains must be chosen for acceptable system performance.

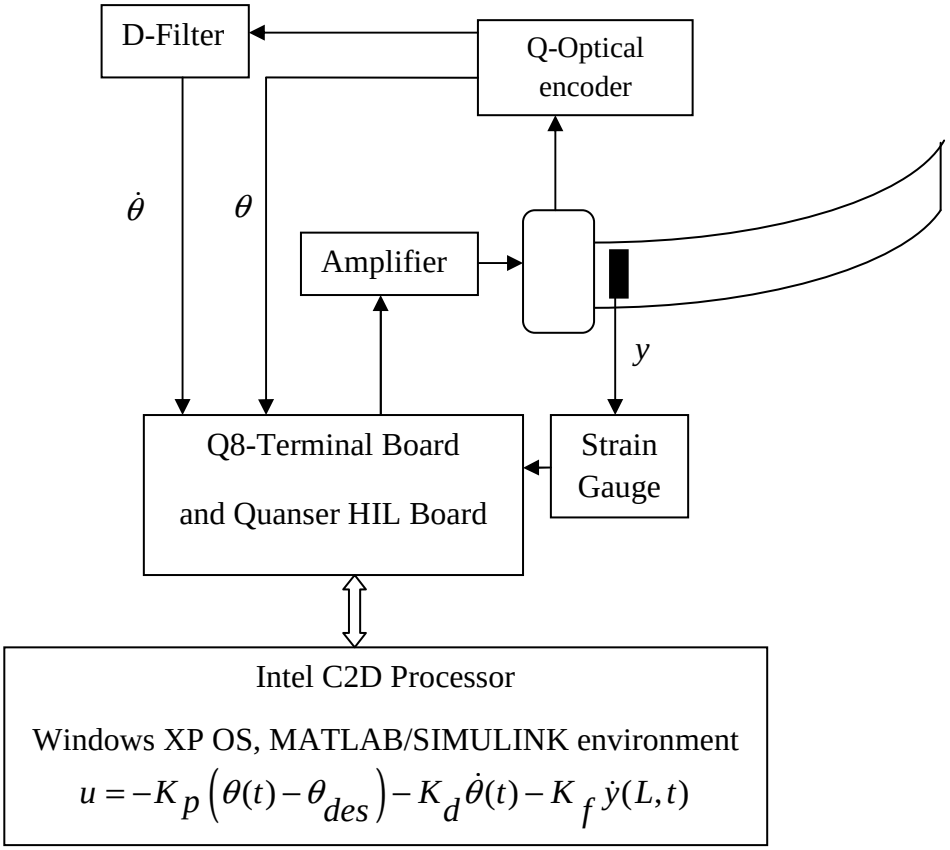

Fig. 4.2 Real-time implementation of controller structure

There are many techniques available for choosing gains of a PD controller provided the system transfer function is known. For a nonlinear system it is cumbersome to find out the gains of controller because of unavailable of any standard tools. The evolutionary techniques are problem independent optimization methods are motivated by living creatures. These techniques optimize parameters by minimizing and/or maximizing a certain function called objective function/fitness function [30]. Here, evolutionary computation techniques have been implemented to find out the optimum gains. Evolutionary technique such as genetic algorithm (GA) is used for optimal tuning of the gains due to its simplicity, straightforward to convergence often lead to satisfactory results. However, in recent years many developments in the areas of evolutionary techniques is reported viz, bacteria foraging optimization (BFO), particle swarm optimization (PSO), ant colony optimization (ACO) etc have proved a better convergence capability than GA is implemented in thrust areas of researches. Here we have implemented BFO for optimization of gains and a comparison with GA is addressed.

4.2.1 Genetic algorithm optimization

Genetic algorithm is a derivative free optimization stochastic optimization method based on natural selection and evolutionary processes. It is a set of systematic steps with each steps are motivated by theory of evolution. It was first proposed and investigated by John Holland in 1975 [31]. Today's human expertise and intelligence is the result of million years of evolution as cited in the theory of evolution proposed by Charles Darwin. He proposed this theory that states only fittest ones survive and passes their

character to the next generation. This idea is motivated and formulated in terms a set of rules by Holland and called it Genetic Algorithm (GA).

These evolutionary algorithms are interest to many researches because of their parallel-search procedure, applicable to both continuous and discrete optimization problems, less chance of getting tapped at local minima/maxima, easily applicable to any set of problems without requiring any knowledge of the system where it is being is used. The basic principle underlies on three steps viz, selection, cross-over and mutation. Initially a set of data are generated randomly called population. Population contain a number of data are called chromosomes; we can say a set of chromosomes form the population. Biologically genes form the core part of the chromosome, or in other word a set of binary bits called gene form the chromosome. A group of genes constituents a single chromosome. Thus if the problem of optimizing needs two parameters to be optimized and we want to have initial population of twenty then we shall have twenty chromosomes with each chromosome contains two genes. It is to be noted that a gene is represented by 4-8 binary bits of chromosome. But in our case we carry out the optimization process using decimal values rather than binary bits without sacrificing accuracy and computational efficiency [21].

Selection: In this step population undergoes a selection procedure. As discussed earlier, GA optimizes a certain fitness function, so each chromosome is associated with its respective fitness value. Here, our problem is to minimize the tip vibration i.e, tip must align along the hub if the vibration is desired to make zero. So the fitness function chosen is modified integral square error (MISE) and is given by

$$F = \int_0^T K\left(p(L,t) - L\theta_{des}\right)^2 dt \quad \text{..... (4.2)}$$

where K is the penalty for overshoot and is given by

$$K = \begin{cases} 1.0 & when \;\; p(L,t) \le L\theta_{des} \\ 10.0 & when \;\; p(L,t) > L\theta_{des} \end{cases}$$

Therefore, fitness function for each chromosome is evaluated using equation (4.2). The chromosomes with minimum fitness value are better ones than those with larger values. The selection criteria is thus to choose first half of members with better fitness values.

Cross-over: Only first half chromosomes undergoes cross-over step. Here chromosomes cross-over each other till population size is reached in order to keep the total population size constant. Any two chromosomes will cross-over or not depends on their cross-over rate. In this step new two offspring's are generated by two parents. In case of binary chromosomes crossover occur at any point of the two chromosomes where they exchange their genetic information and pass it to their child. Instead that in decimal numbers each parent contributes to its subsequent generation.

$$Child1: \begin{cases} K_p = c * K_{p1} + (1-c) * K_{p2} \\ K_d = c * K_{d1} + (1-c) * K_{d2} \\ K_f = c * K_{f1} + (1-c) * K_{f2} \end{cases} \quad \text{..... (4.3)}$$

$$
Child2:\begin{cases} K_p = (1-c)*K_{p1} + c*K_{p2} \\ K_d = (1-c)*K_{d1} + c*K_{d2} \\ K_f = (1-c)*K_{f1} + c*K_{f2} \end{cases} \quad \ldots\ldots\ldots\ldots\ldots\ldots\ldots\ldots\ldots\ldots\ldots \text{(4.4)}
$$

where c is a random number and we have chosen 0.8 so that each parent will pass the genetic information to a particular child. Subscript 1 and subscript 2 denote parent 1 and parent 2 respectively.

Mutation: In cross-over the genetic information is passed to their posterity. However in some cases it is found some genetic information of parent is lost due to crossover and good parents might result in offspring's with less chance of survival. This occurs in biological evolution and hence it is also imitated here mathematically. Each new chromosome undergoes mutation if it satisfies certain mutation rate. In all cases it is common sense to select the mutation rate very low and in this optimization process we have taken mutation rate to be 0.1. The offspring's undergoing mutation results in

$$
\begin{aligned} K_p &= K_p + (m_1 - 0.5)*2*K_{p\_max} \\ K_d &= K_d + (m_2 - 0.5)*2*K_{d\_max} \\ K_f &= K_f + (m_3 - 0.5)*2*K_{f\_max} \end{aligned} \quad \ldots\ldots\ldots\ldots\ldots\ldots\ldots\ldots\ldots\ldots \text{(4.5)}
$$

where m_i are the random constants of three gains and are taken as 0.6 for three gains and K_{p_max} is the maximum allowable changes during mutation in K_p and so on. The overall procedure is shown in flow chart in Fig.4.3.

In most derivative free optimization procedure it is quite important to choose initial population and maximum number of generation. Equations (4.2)-(4.6) are repeated

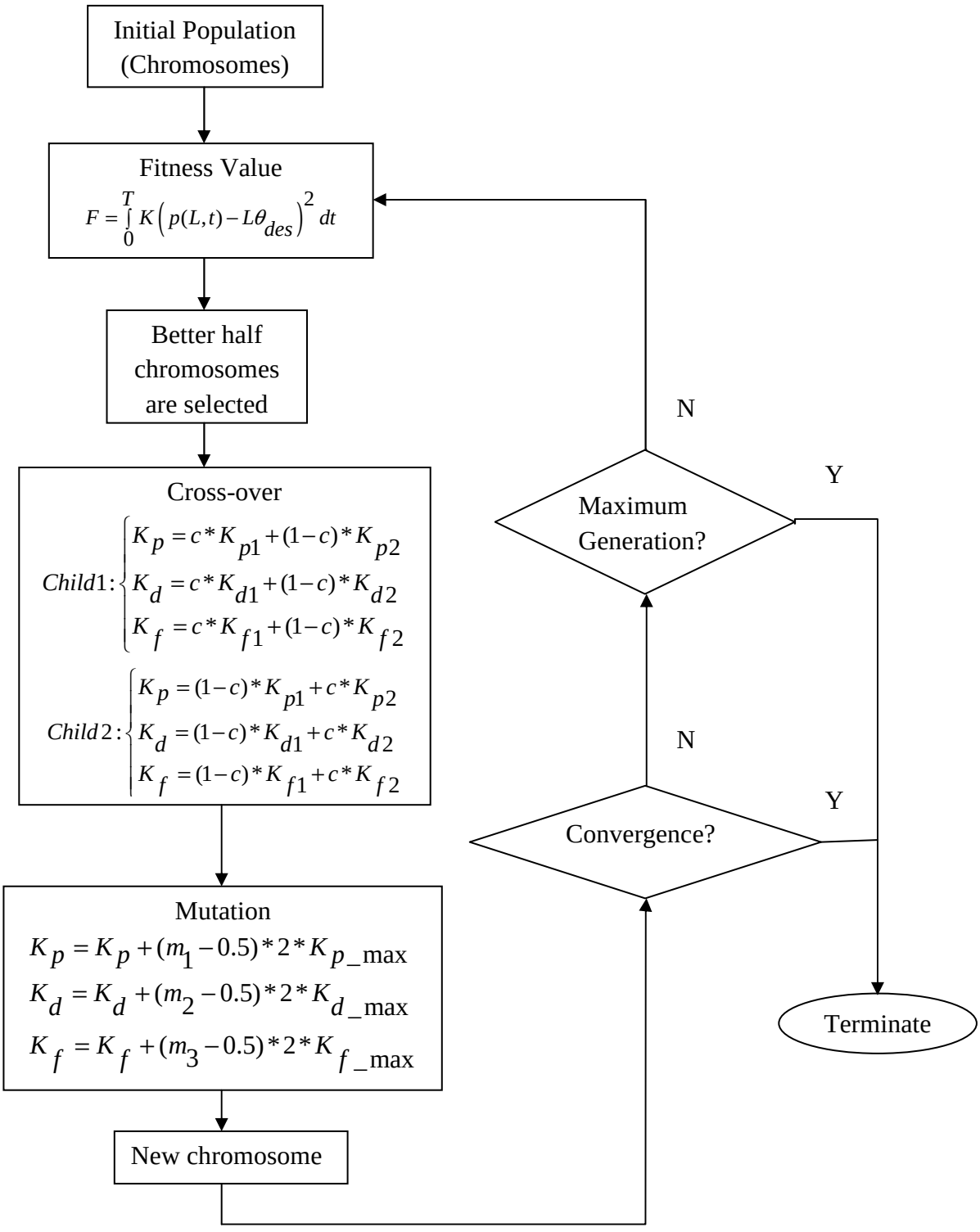

Fig. 4.3 Flow chart of genetic algorithm

for a till the maximum number of generation is reached or whichever is earlier till a termination criteria is met. One must be careful while choosing initial population because large population may lead to longer time to converge and vice versa. On the contrary we can say engineering judgment must be made to maximum number of generation otherwise GA would be repeated even though all the chromosomes have converged at some generation enough earlier now to terminate the process. Of course choosing between number of generation and population is not unique; rather it exclusively relies on the problem. However it is of not much concern to the user once a suitable termination criterion is met. One may choose the termination criteria as; if no change in fitness function occurs appreciably during some generation (say for 30 generation) the optimization process is terminated. Here we have taken 50 chromosomes per population, 0.0001 as tolerance for fitness function must satisfy to terminate the process.

4.2.2 Bacterial foraging optimization

Bacterial Foraging Optimization (BFO) is another derivative free optimization method proposed by Kevin M. Passino [27] in 2002. This algorithm represents behavior of bacteria (*E. coli*) over a landscape of nutrients. Many researchers have studied the behavior of *E. coli* and its other species especially their locomotion, generation during their life cycle. Very interesting features have been observed how it moves towards non noxious environment without having any knowledge on the environment. *E. coli* is best suitable microorganism whose life cycle can be understood easily. It has a plasma membrane, cell wall, a nucleon and a numerous flagellum over its body used for locomotion. The bacteria normally wanders for food patches over a medium and it

randomly moves in random direction. It continues its movement in a particular direction if nutrient gradient increases otherwise it tumbles. This step is called chemotaxis step of bacteria. While it is moving towards the food patch it sends some attractant secretions which enable nearby bacteria to move towards food patch. However the bacteria are also very cautious about its own life and it does not allow all bacteria to move towards food patch that will create a noxious environment for its own life. So it also secretes repellent signals which will resist large number of bacteria affected by its attractant signals. Such behavior is represented as swarming. Once this is over they undergo reproduction step in which bacteria in noxious environment dies and those in non noxious environment survives and reproduces bacteria at their same location to keep total number bacteria constant. It is natural some bacteria still in non noxious environment dies and/or totally eliminated. This is called elimination and dispersal step.

Very important and innovation step of *E. coli* is the chemotaxis step thereby the bacteria undergoes changes with respect to both position and time. Now the obvious question is how does a bacterium move ahead or backward? It is said earlier *E. coli* have numerous flagella that is responsible for locomotion. Each flagella is left-handed helix, when it rotates counterclockwise as viewed from free end of flagella looking towards the cell it creates a force against the cell so that the bacterium moves forward. However each bacterium do have a large number of flagella and their cumulative effect of pushing the bacterium forward would make the bacterium to swim forward. This is shown clearly in Fig.4.4. On the other hand when flagella rotate clockwise the net effect of flagellum is to pull the cell towards itself.

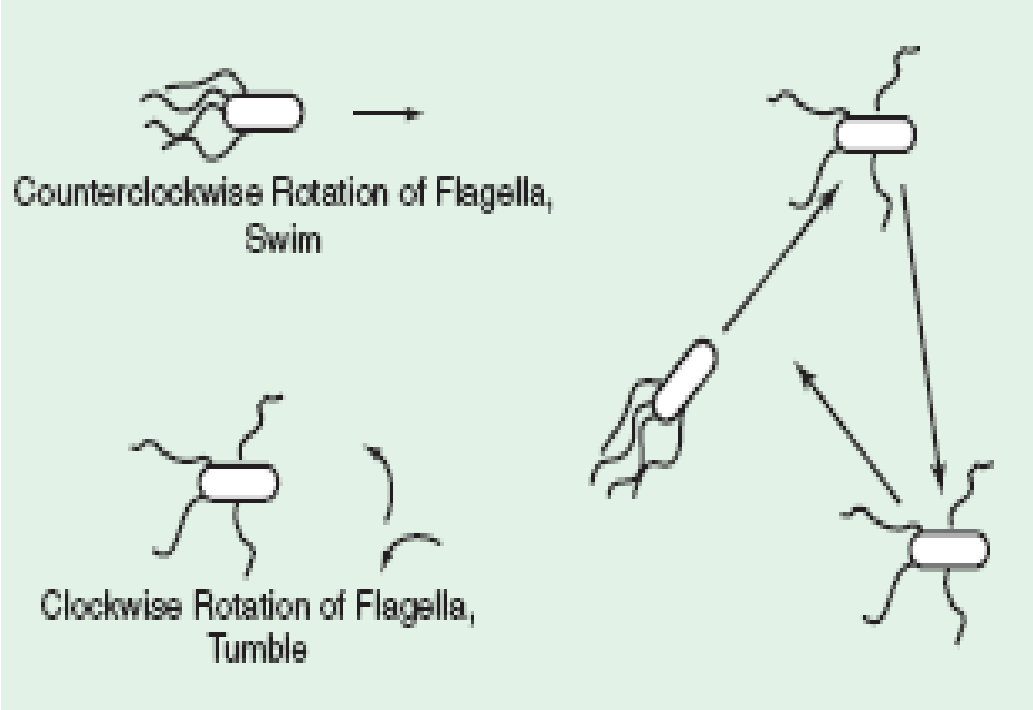

Fig. 4.4 Bacteria locomotion due to flagella rotation

Presence of large number of flagella will pull the cell in their respective direction making the bacteria to tumble i.e, it cannot decide whether to swim or run. The details of each step with relevant to flexible robot are discussed below. In general we represent each bacterium as $\theta^i(j,k,l)$ in following description with superscript represents i^{th} bacterium undergoing j^{th} chemotaxis step, k^{th} reproduction step and l^{th} elimination and dispersal step.

Chemotaxis: Initially a bacterium population is created randomly. In our problem each bacterium constituent three parameters representing three gains of the controller. First in this step the fitness value at each bacterium location is found out by suitably selecting a fitness function. Here same fitness function (F) MISE is chosen for comparison purpose with GA. Each bacterium is allowed to move in a certain random

direction and again fitness value denoted as F_{new} is calculated. If $F_{new} < F$ is satisfied then bacterium moves another step in that direction till a maximum number of swim step is reached. It is obvious choice that to choose maximum swim step in a chemo taxis stage less than the number chemotaxis step. However if noxious environment is noticed the bacterium tumbles between swim and run. Mathematically it can be represented as suppose the bacterium $\theta^i(j,k,l)$ is undergoing j^{th} chemo taxis step then swim of the bacterium in a random direction $\phi(i)$ with chemo tactic step $C(i) > 0$

$$\theta^i(j+1,k,l) = \theta^i(j,k,l) + C(i)\phi(i) \ldots\ldots\ldots\ldots\ldots\ldots\ldots\ldots\ldots\ldots \quad (4.6)$$

The random direction is of unit magnitude can be represented as $\phi(i) = \Delta(i) \Big/ \sqrt{\Delta^T(i)\Delta(i)}$ where $\Delta(i)$ is generated randomly. While the bacteria moves with each chemo tactic step fitness function is evaluated to calculate nutrient concentration at each position they are traversing. This is repeated for all bacteria (say S is number of bacteria in a population)

Swarming: In each chemotaxis step the bacteria moves in a particular direction if the favorable nutrient is detected. While doing so, each bacteria secrets some attractant and repellent signals which allow the nearby bacteria to move to nutrient medium. This stage ensures overall convergence of population which is the key feature of gradient free optimization methods. This can be understood as large number of bacteria swarming in container with nutrient kept at the centre. If one bacterium detects food concentration and it signals to nearby bacteria then a group of bacteria would converge to centre rather than a single bacteria would have moved. This increase converge rate of

overall population and reduces optimization time which is very crucial part of bio-inspired optimization methods. That is fitness value at current location of bacteria is affected by the presence of nearby bacteria. Mathematically it can be represented as

$$F = \sum_{i=1}^{S}\left(d_{attract} \exp\left(-w_{attract} \sum_{m=1}^{p}\left(\theta_m - \theta_m^i\right)^2 \right)\right) + \sum_{i=1}^{S}\left(h_{repellent} \exp\left(-w_{repellent} \sum_{m=1}^{p}\left(\theta_m - \theta_m^i\right)^2 \right)\right) \quad \text{..... (4.7)}$$

where p is the number of parameter to be optimized and other parameters carry their respective meaning.

Reproduction: It is health assessment step where better bacteria survive and higher fitness value members die. Here half of the bacteria of population with least fitness value survive and rest worst bacteria are killed. It is to be noted that the new bacteria are generated at same location with that of parent for better convergence.

Elimination and Dispersal: It is very intuitive to living being that calamities often causes best member also to quit and bacteria are of no exception. When bacteria move in a certain nutrient media it enters medium with different environment conditions. Suppose bacteria moving in stomach experiences different pH conditions which decide their adaptability to the environment. In real situation some bacteria die and some survive even though they belong to same species. In the algorithm step they are randomly destroyed; however in order to keep the total number of bacteria constant, same numbers of bacteria are generated randomly at random locations. The complete procedure is shown in flow chart in Fig.4.5.

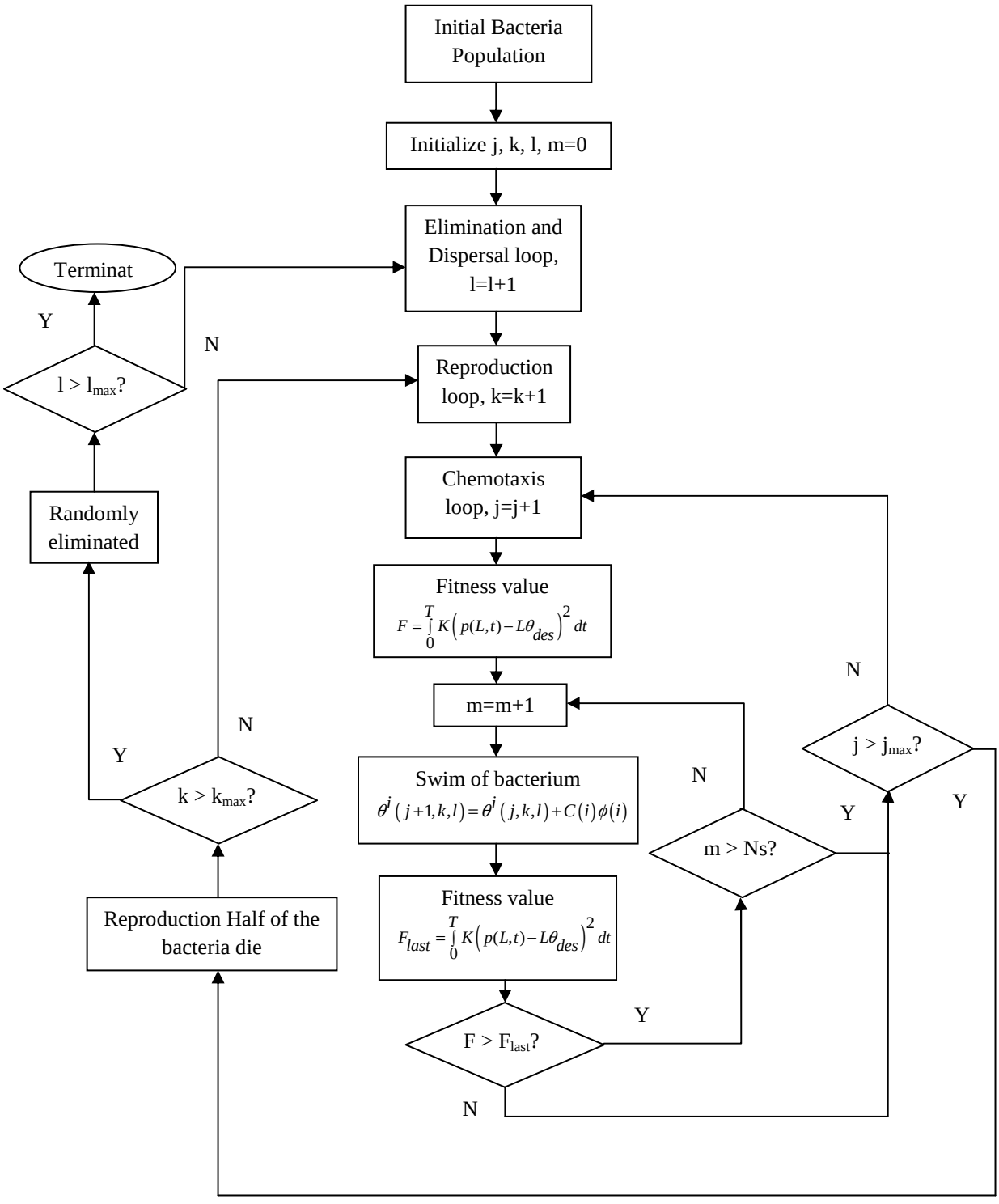

Fig. 4.5 Flow Chart of Bacterial foraging optimization method

4.3 Simulation results

To carry out the study of effectiveness of the application of evolutionary techniques in the tip feedback controller, numerical simulation is carried out. At first GA is applied to tune the gains of the controller. Here in GA optimization technique, we have chosen fifty chromosomes per population randomly at the starting of the process. This initial population is chosen randomly but within some specific domain. As we have three gains so there are three genes in a single chromosome. It must be kept in mind that throughout the process decimal values are used rather than binary bits as is the case in conventional GA. The different ranges of gains are taken as 0-20, 0-5 and 0-20 for K_p, K_d and K_f respectively. The cross-over and mutation rates are taken as 0.9 and 0.1 respectively. We expect that better parents will be mostly for the next generation.

At start of the optimization process the fitness value of each chromosome is evaluated as per equation (4.2). The fitness value is evaluated for 2 sec (T=2 sec) because the maximum time to settle the tip at final position $L\theta_{des}$ is chosen as 2 sec. The fitness function in this case is taken as MISE to let the tip must not give large overshoot while minimizing the rise time. In mutation the maximum allowable changes in the K_p, K_d and K_f are 0.8, 0.9 and 1 respectively. The simulation is carried out for a maximum generation of 100. However, it is not a wise decision to run the process for 100 generation because of time and resource are not properly utilised. Hence it is imperative to use a termination criterion from the practical point of view. Particularly in this problem the variation of fitness function is used for termination criterion. If the fitness function

value doesn't change much or it is within the tolerance value over a certain number of generation then we may terminate the process. The fitness function plot is shown in Fig.4.6.

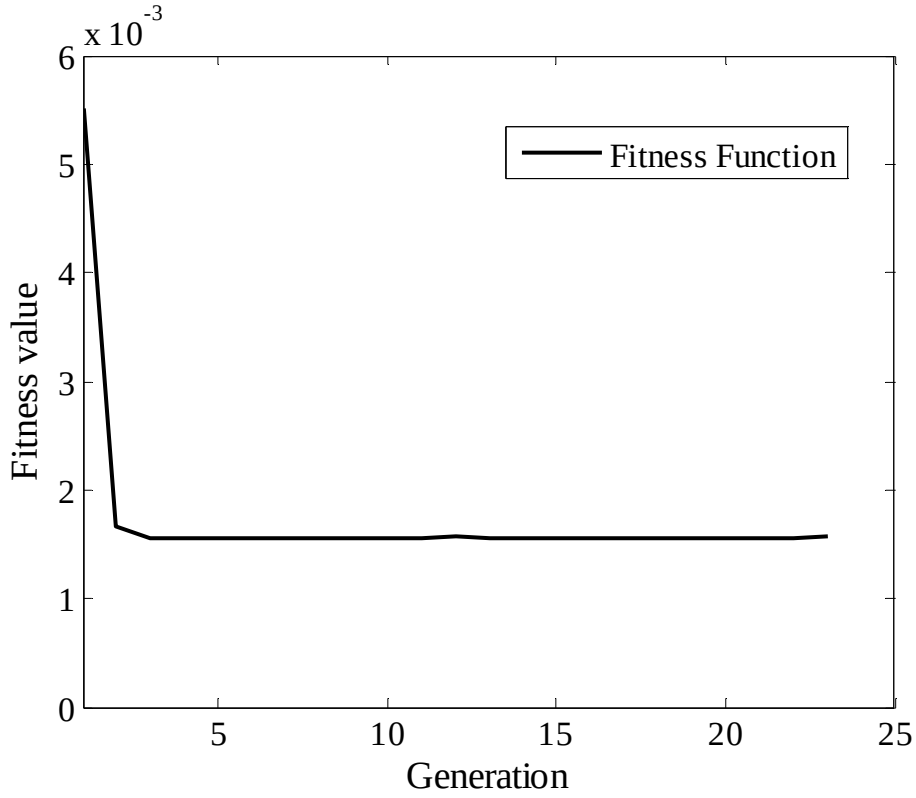

Fig. 4.6 Fitness function of GAO method

Here best individual is picked for which the fitness value is plotted. In the case gradient free optimization processes always first position occupied by best individual and. It is shown that at 23rd generation the process is terminated as it met the termination criterion. Almost at 3rd generation the fitness value becomes the order of 10^{-3} indicating the fast convergence rate of population. The corresponding gains i.e, first chromosome throughout the optimization process is shown in Fig.4.7. From this figure, we can observe that first chromosome doesn't show much variation after 3rd generation and it remains constant throughout the optimization process.

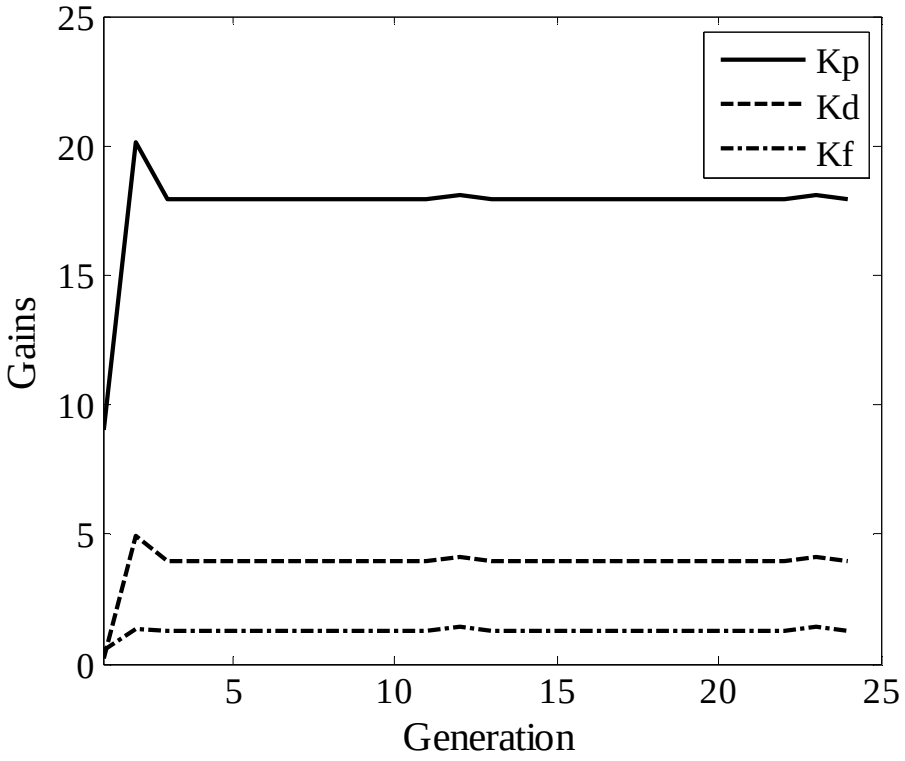

Fig. 4.7 Gains of GAO method

The gains thus obtained at last generation are the optimum gains tuned by GA. The final gains we obtained using GA tuning are 17.9569, 3.9904 and 1.2505 for K_p, K_d and K_f respectively. These gains are used in the controller given by equation (4.1) and numerical simulation carried out to study the effectiveness of the GA tuning tip feedback controller. The following figures 4.8 (a)-(c) show the hub angle, tip deflection and tip trajectory variation with the GA tuned gains is shown.

The desired hub angle of the motor is set at 0.5 rad and tip feedback controller with GA tuned gains is implemented to position the tip of the flexible link robot at desired tip position $L\theta_{des}\left(=0.11\,m\right)$. The hub reached at 0.5 rad in 1.6 sec but considering settling

time of the hub to settle within ±2% tolerance band of 0.5 rad it requires 0.95 sec. Tip deflection is also suppressed at its first half cycle.

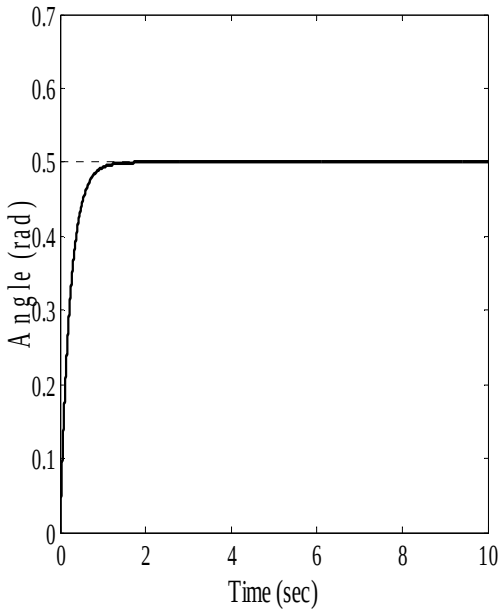

Fig. 4.8 (a)

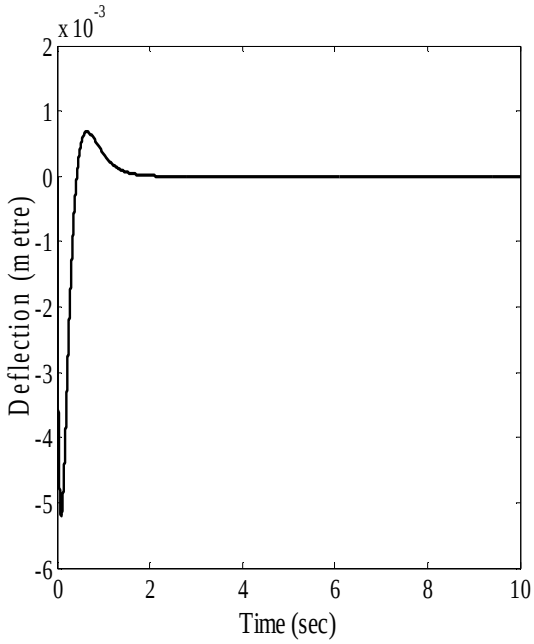

Fig. 4.8 (b)

The initial undershoot (Fig.4.8 (b)) is due to the non-minimum phase characteristic. The tip trajectory during the regulation problem is plotted in Fig.4.8 (c). The settling time for the tip is also found out to be 0.95 sec. Very negligible overshoot of the order 10^{-3} and smooth tip positioning is achieved by this GA tuning tip feedback controller. However the tip reaches the final position 0.11 m at nearly 1.7 sec. It can be said at this point that with incorporating evolutionary techniques into the simple joint PD tip feedback controller the performance of the controller is improved significantly because in conventional tuning methods no optimal gains are chosen.

With clearly examining the performance of GA tuning controller gains and availability of some improved gradient free optimization method at hand we can expect better results than conventional methods. Here we exploited another technique BFO for

tuning the gains. To compare the potential of BFO over GA we need some common bases like same fitness function, same number of bacteria etc and see their convergence rate.

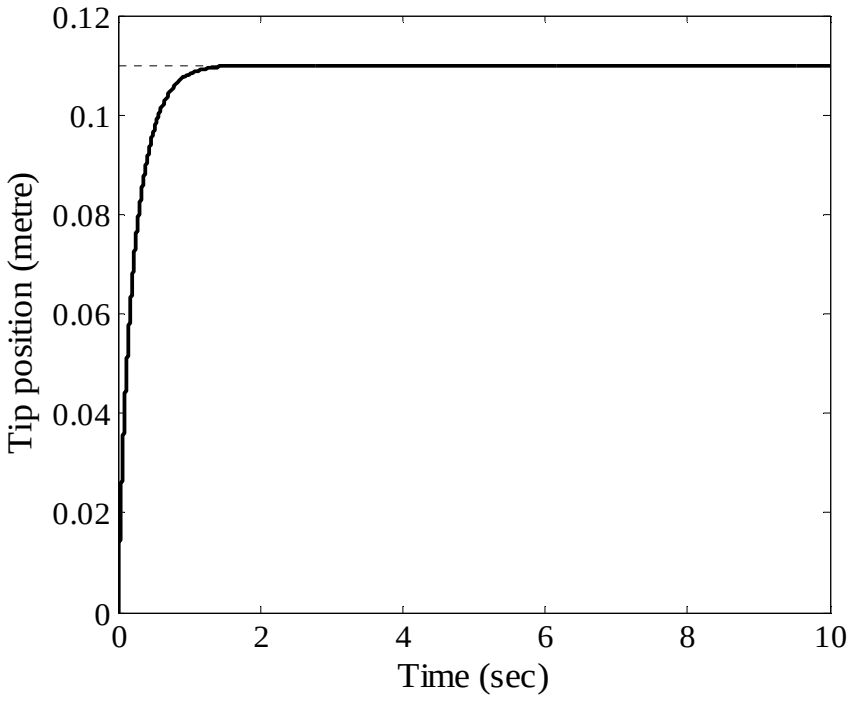

Fig. 4.8 (c)

Fig. 4.8 Simulation results with GA optimized gains (a) Hub angle, (b) Tip deflection and (c) Tip trajectory

The different parameters chosen for BFO technique are 50 bacteria with each containing three parameters, 10 chemo taxis steps with a maximum four swim step in each chemo tactic step, two reproduction and elimination and dispersal steps. The elimination and dispersal probability is taken as 0.25. The fitness function plot is shown in Fig.4.9 to measure the accuracy of the method. The fitness value obtained of the order of 10^{-4} compared to GA where it is of order10^{-3}. Therefore the gains tuned by BFO are better tip positioning capability than GA tuning gains. Here, in abscissa labels the total number of chemo taxis, reproduction and elimination and dispersal steps. The fitness function shown here is the track of best bacteria converging towards the non noxious environment.

The movement of best bacteria is plotted in fig.4.10 where it always moves towards the optimum solutions. Gains don't change much after 25 stages of the bacteria.

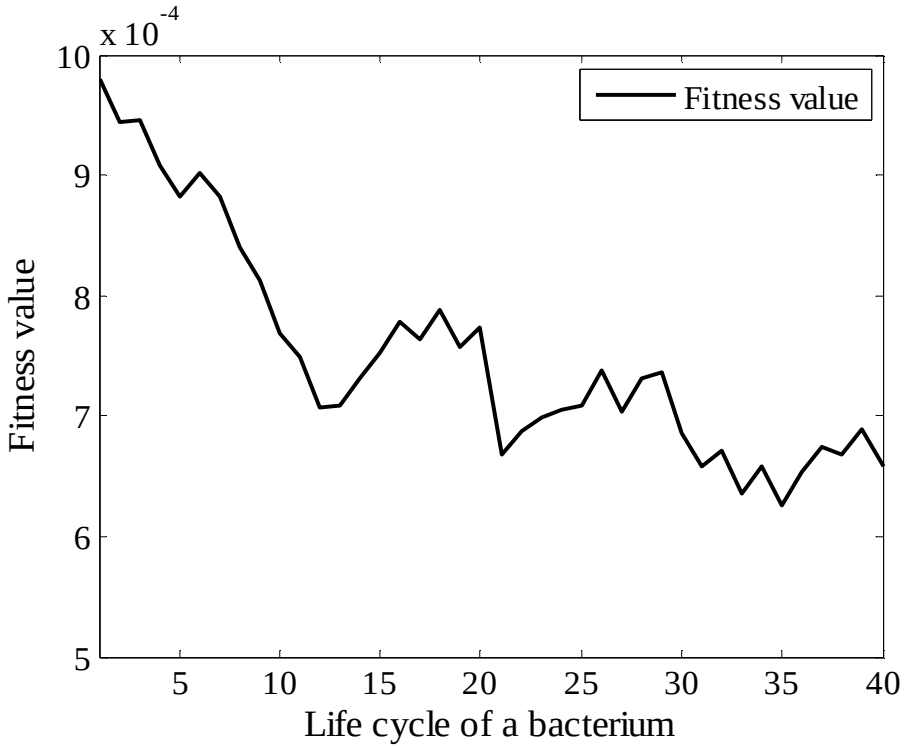

Fig. 4.9 Fitness function BFO method

The final gains obtained are used in the controller to study the effectiveness of the BFO tuned gains. The final gains we obtained using GA tuning are 17.3955, 1.8010 and 17.6588 for K_p, K_d and K_f respectively. The initial bacteria population is generated randomly within the same domain as that of GA population. It is to be noted in the BFO method we have not considered swarming mechanism of bacteria for each in optimization; however inclusion of swarming signal will make the process to convergence faster than that of without swarming mechanism. Comparison of Figs. 4.11 (a)-(c) with Figs. 4.8 (a)-(c) shows quite improvements in the performance of controller in terms of settling time, rise time etc. The settling time for hub angle to settle within the

±2% band of the final value is 0.4 sec. Similarly it is for tip of the flexible link robot is nearly 0.5 sec which indicates more improvement is reported in the case of BFO tuned gains. The deflection of the tip is also suppressed in first cycle of vibration. A comparison of study of both the tuning is reported later section of this chapter.

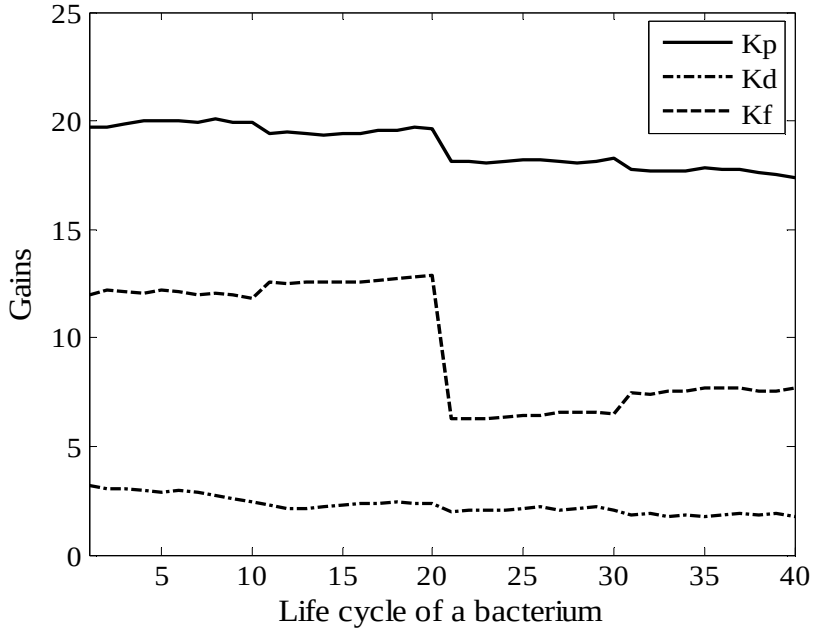

Fig. 4.10 Gains of BFO method

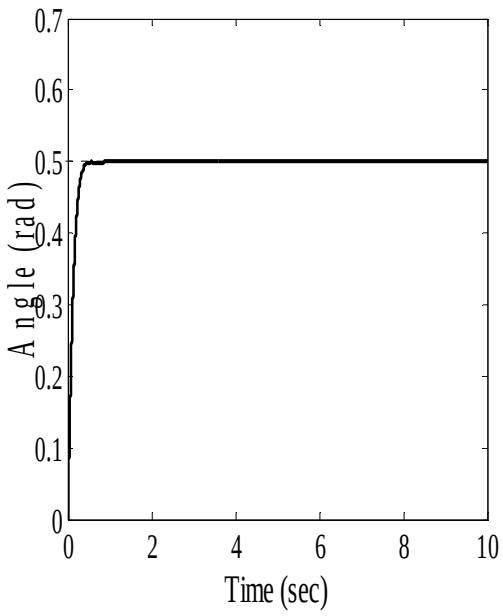

Fig. 4.11 (a)

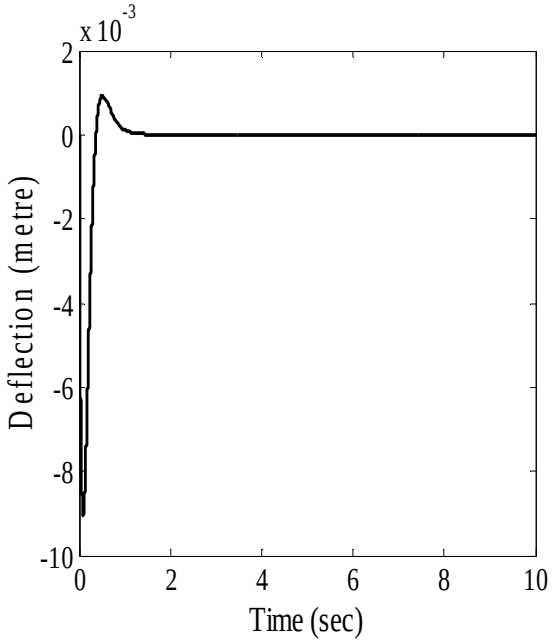

Fig. 4.11 (b)

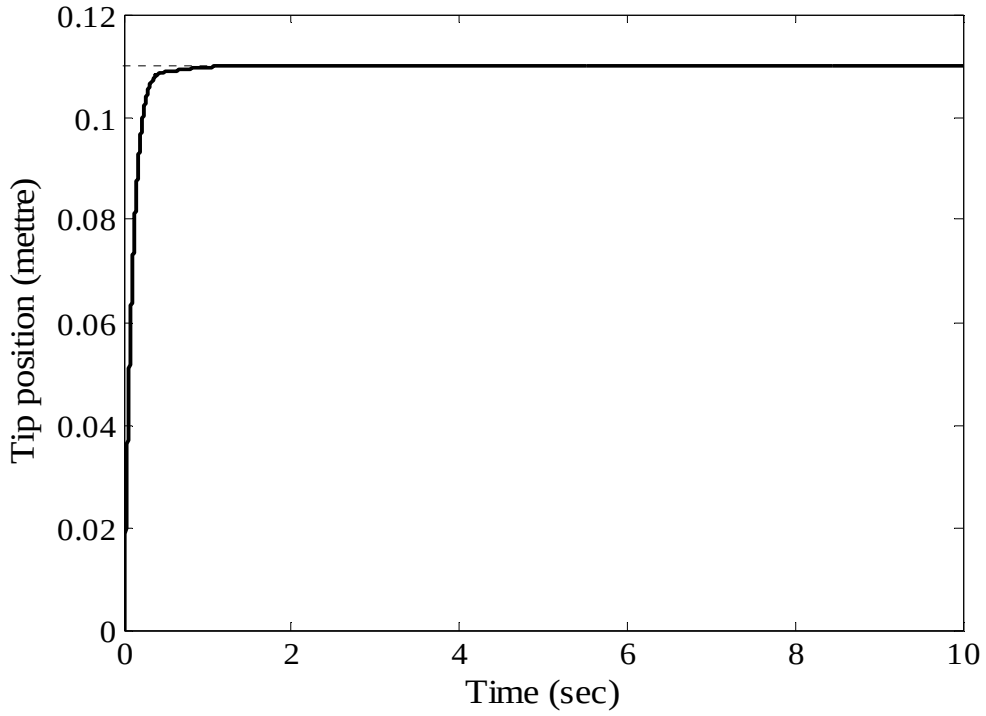

Fig. 4.11 (c)

Fig. 4.11 Simulation results with BF optimized gains (a) Hub angle, (b) Tip deflection and (c) Tip trajectory

4.4 Experimental results

To study the practical aspects of the controller, gains obtained by GA and BFO tuning are implemented in real time test bed and compared with simulation results. The hub angle, tip deflection and tip position to a final tip position of 0.5 rad is shown in Fig.4.12 (a)-(c). The tip undershoots initially with very large magnitude but after that is suppressed to zero. Hub angle and tip position finally settles at 0.5 rad and 0.11 m respectively. Tip of the robot rises smoothly without actuating the vibration. It is to be noted that a compromise has to be made between rise time and settling time with no vibration of tip.

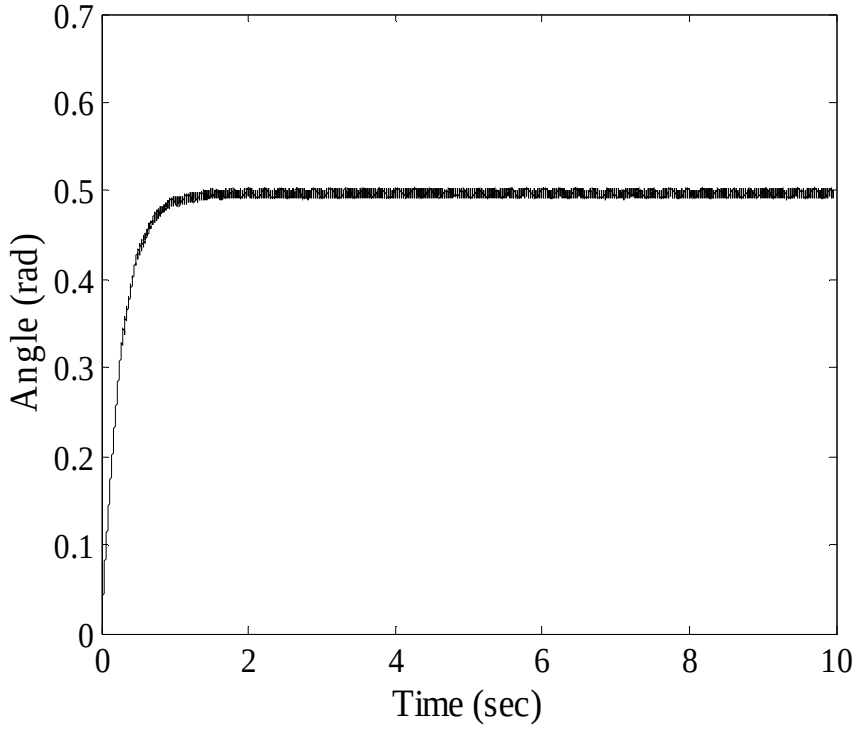

Fig. 4.12 (a)

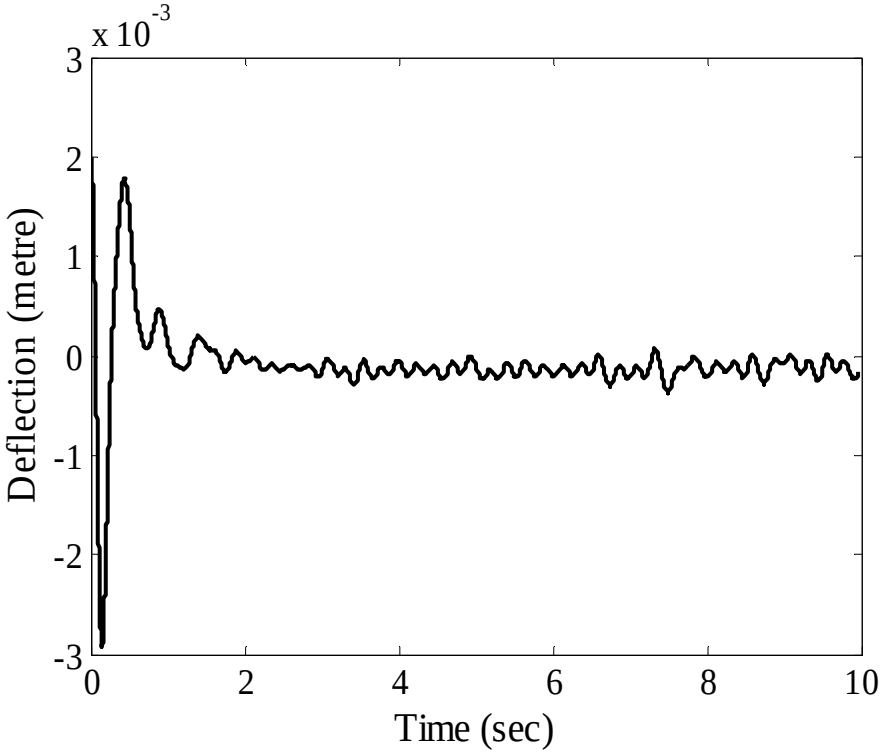

Fig. 4.12 (b)

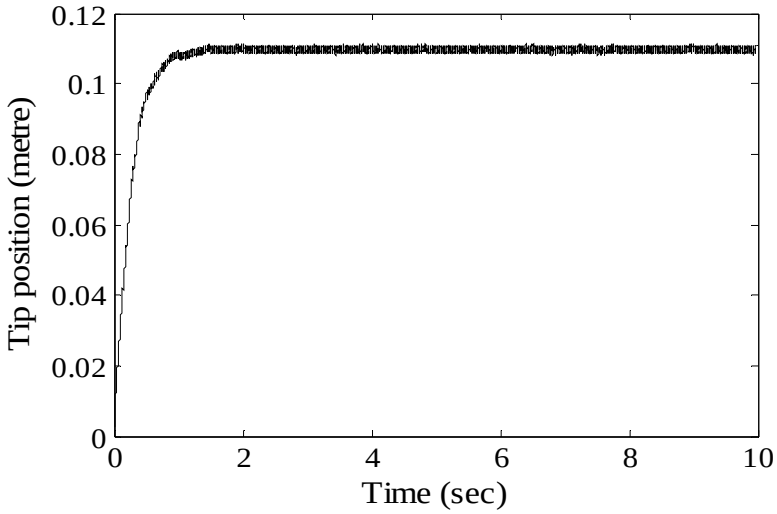

Fig. 4.12 (c)

Fig. 4.12 Experimental results with GA optimized gains (a) Hub angle, (b) Tip deflection and (c) Tip trajectory

The responses are similar to that obtained in simulation studies. The settling time for both hub angle and tip is found to be 0.95 sec same as of simulation results. Here vibration is damped out in first cycle however noise amplifying signals results in very small magnitude oscillation in hub angle and tip trajectory with GA tuned gains.

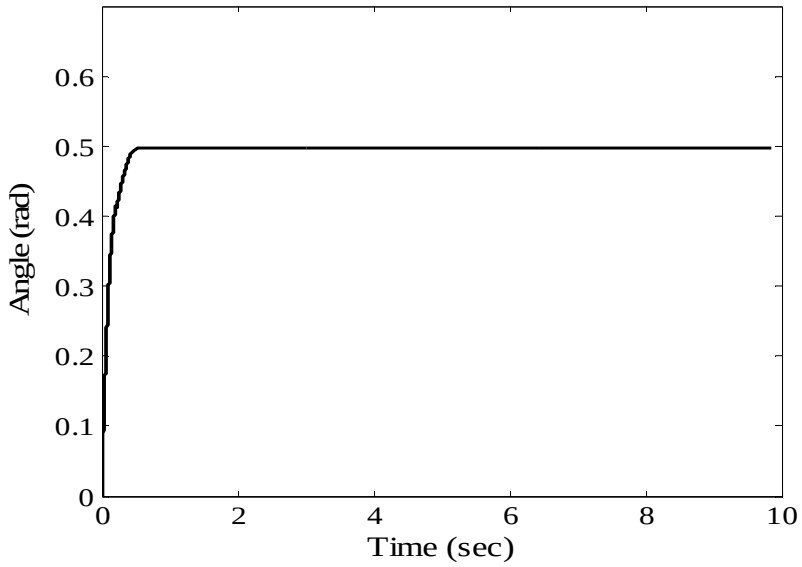

Fig. 4.13 (a)

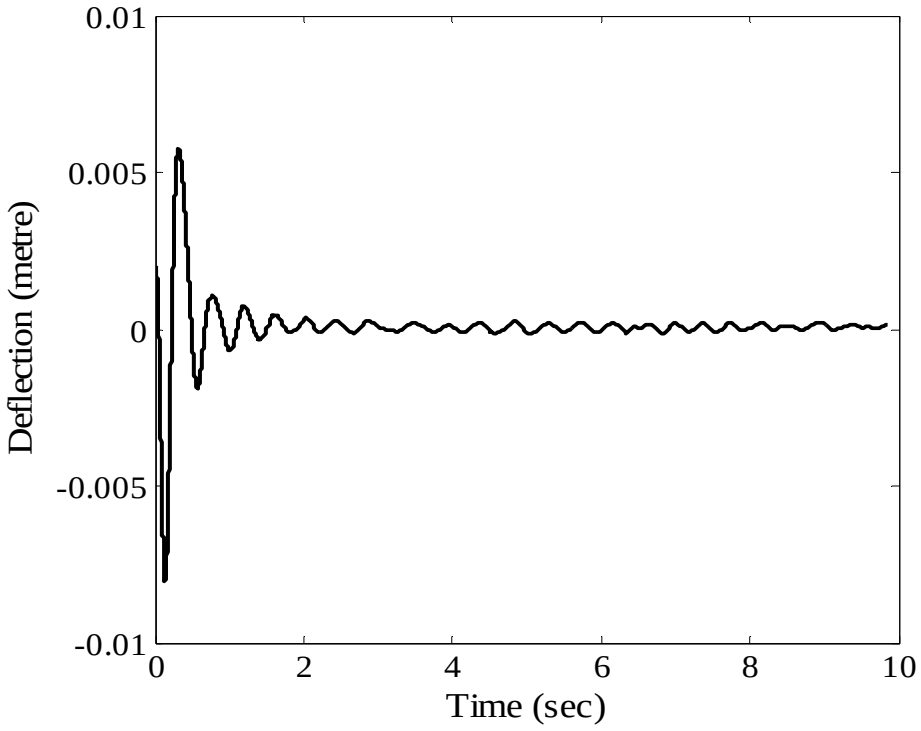

Fig. 4.13 (b)

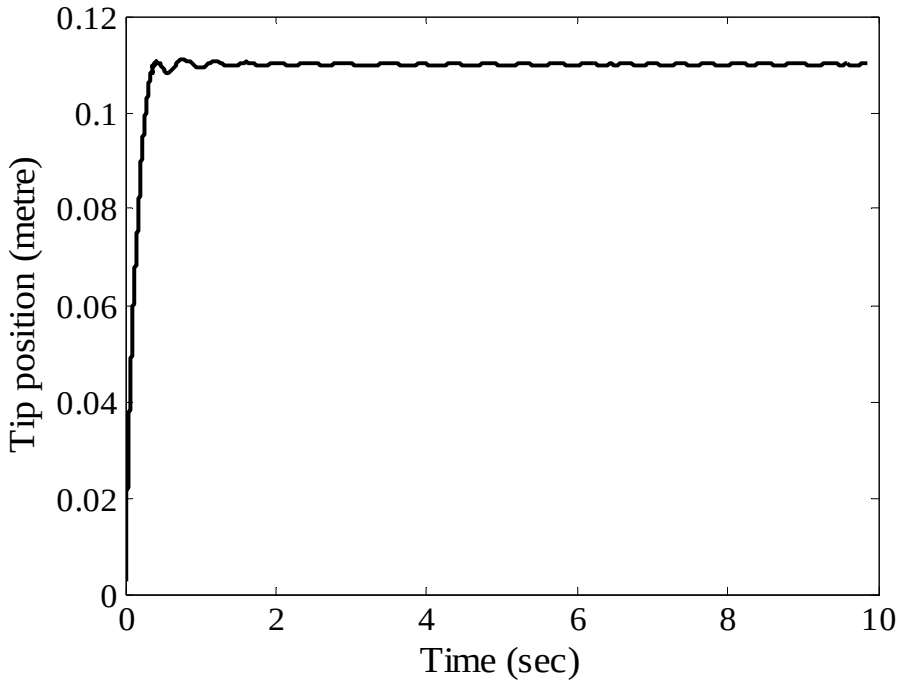

Fig. 4.13 (c)

Fig. 4.13 Experimental results with BF optimized gains (a) Hub angle, (b) Tip deflection and (c) Tip trajectory

TABLE 4.1 PERFORMANCE MEASURES OF THE TIP FEEDBACK CONTROLLER WITH GA & BFO TUNING

Performance Indices	GA tuned gains	BFO tuned gains
Settling time	0.95 sec	0.4 sec
Rise time	1.3 sec	0.38 sec
Peak time	1.5 sec	0.41 sec
Overshoot	0.91%	0.45%
Steady state error	0	0

The hub, tip deflection and tip trajectory for BFO gains are shown in Fig.4.13 (a)-(c).The tip response of BFO tuned gains is much faster than GA tuned gains (Fig.4.13(c)). The tip settles within $\pm 2\%$ band of steady state response in 0.4 sec without any high frequency vibrations. Due to fast response the tip undershoots with large magnitude but it subsides within 1.5 sec. Table 4.1 shows the performances of the both the tuning methods. Both these methods result in overshoots but within the system requirements. Looking at both of these methods the application of evolutionary computing techniques for gain optimization results in the optimal selection of gains than stable gains as in the case of conventional design methods where design is primarily based on the stability rather than optimal performances.

4.5 Summary

Section 4.1 reviews some of earlier developments in the controller. In section 4.2 tip feedback controller is proposed with evolutionary techniques employed to tune the gains of the controller. The details of genetic algorithm and bacteria foraging optimization are presented with relevance to flexible robot. The following two sections discuss the performance of these two methods.

Chapter 5

Conclusions and Suggestions for Future Work

5.1 Conclusions

In this the chapter we discuss many advantages and disadvantages associated with the controller even some of the future challenges and scope for further development. The dynamics of the flexible link robot is discussed in chapter 3 where AMM and FEM models are obtained. The basic difference in both of these models are deflection in AMM is obtained in terms of number of modes while in FEM the cumulative deflections at nodes of elements give the deflection of tip of the robot. Deflection in FEM model is more practical signification than AMM model however assumed mode model is very explicit, straightforward. The model validation figures show the results of AMM are very appreciable to real time, but for multilink FEM model would be useful in design of the controller.

During the design of controller non minimum phase characteristic has not been taken into consideration because we concentrate only at final position control. Of course that the simple joint PD controller won't take care of such problem for which some other complex controller may be appropriate. However in the tracking problem the tip feedback

controller would have a delayed response for which some better controller can be designed. But for tip position problem this controller is very effective for placing the tip at its desired position. The simulation results are shown for GA and BFO tuned gains to study the performance of the controller. To study the practical applicability of the proposed controller real time experimental study is carried out. Thus it can be said that the controller can be used as far as tip position is concerned.

5.2 Suggestions for future work

The proposed work in this thesis is for single link flexible manipulator which can be extended in future perspective. These are some suggestions made for reference.

- The modeling techniques can be extended to two link manipulator with incorporating actuator dynamics in both assumed mode model and finite element model.
- This controller is very easy to implement that only it needs the computation of gains by offline method and then using it in real time. Moreover no complexities are present like other controller so it can be extended to a multilink flexible manipulator.
- Some online tuning methods can be employed to vary the gains of the controller in order to make the system unaffected under any parameter variation.

References

[1] S. K. Dwivedy and P. Eberhard, "Dynamic analysis of a flexible manipulator, a literature review," *Mech. Mach. Theory.,* vol. 41, pp. 749-777, 2006.

[2] G. G. Hastings and W. J. Book, **"**A linear dynamic model for flexible robotic manipulators," *IEEE Contr. Syst. Mag.,* vol. 7, no. 1, pp. 61-64, 1987.

[3] P. K. C. Wang and J. D. Wei, "Vibration in a moving flexible robot arm," *J. Sound and Vibrat*., pp. 149–160, 1987.

[4] D. Wang and M. Vidyasagar, "Transfer functions for a single flexible link," *Proc. IEEE Int. Conf. Robotics and Automation,* pp.1042–1047, 1989.

[5] R.J. Theodore and A. Ghosal, "Modeling of flexible-link manipulators with prismatic joints," *IEEE Trans. Syst., Man, Cybern., pt. B,* vol. 27, no. 2, pp. 296–305, 1997.

[6] D. Wang and M. Vidyasagar, "Modelling a class of multilink manipulators with the last link flexible," *IEEE Trans. Robot. Automat.,* vol. 8, no. 1, pp. 33–41, 1992.

[7] A. De Luca and B. Siciliano, "Trajectory control of a nonlinear one-link flexible arm," *Int. J. Contr.,* vol. 50, no. 5, pp. 1699–1715, 1989.

[8] A. De Luca and B. Siciliano, "Closed-form dynamic model planar multilink lightweight robots," *IEEE Trans. Contr. Syst. Technol.,* vol. 21, no. 4, pp. 826-839, 1991.

[9] J. M. Martins, Z. Mohamed, M. O. Tokhi, J. S. D. Costa and M. A. Botto, "Approaches for dynamic modelling of flexible manipulator systems," *Proc. IEE Control Theory Appl.,* vol. 150, no. 4, 2003.

[10] M. O. Tokhi and Z. Mohamed, "Finite element approach to dynamic modelling of a flexible robot manipulator: performance evaluation and computational requirements," *Commun. Numer. Meth. Engng.,* vol. 15, pp. 669-678, 1999.

[11] S. S. Ge, T. H. Lee and G. Zhu, "Improving regulation of a single-link flexible manipulator with strain feedback," *IEEE Trans. Robot. Automat.,* vol. 14, no. 1, pp. 179–185, 1998.

[12] S. S. Ge, T. H. Lee and G. Zhu, "A nonlinear feedback controller for a single-link flexible manipulator based on a finite element model," *J. Robot. Syst.*, vol. 14, no. 3, pp. 165-178, 1997.

[13] B. Subudhi and A. S. Morris, "Dynamic modelling, simulation and control of a manipulator with flexible links and joints," *Robotics and Autonomous. Syst.*, vol. 41, pp. 257-270, 2002.

[14] H. Geniele, R. V. Patel and K. Khorasani, "End-point control of a flexible-link manipulator: theory and experiments," *IEEE Trans. Contr. Syst. Technol.*, vol. 5, no. 6, pp. 556-570, 1997.

[15] A. De Luca and B. Siciliano, "Inversion-based nonlinear control of robot arms with flexible links," *J. Guid. Contr. and Dynam.*,vol. 16, no. 6, pp. 1169-1176, 1993.

[16] M. Moallem, R. V. Patel and K. Khorasani, "Nonlinear tip-position tracking control of a flexible-link manipulator: theory and experiments," *Automatica*, vol. 37, pp. 1825-1834, 2001.

[17] W. J. Wang, S. S. Lu and C. F. Hsu, "Experiments on position control of a one-link flexible robot arm," *IEEE Trans. Robot. Automat.*, vol. 5, no. 3, pp. 373–377, 1989.

[18] Z. Su and K. Khorasani, "A neural-network-based controller for a single-link flexible manipulator using inverse dynamics approach," *IEEE Trans. Ind. Elect.*, vol. 48, no. 6, pp. 1074-1086, 2001.

[19] B. Subudhi and A. S. Morris, "Soft computing methods applied to the control of a flexible robot manipulator," *J. Appl. Soft Computing.*, vol. 9, no. 1, pp. 149-158, 2009.

[20] Y. Aoustin, C. Chevallereau, A. Glumineau, and C. H. Moog, "Experimental results for the end-effector control of a single flexible robotic arm," *IEEE Trans. Contr. Syst. Technol.*, vol. 2, no. 4, pp. 371-381, 1994.

[21] S. S. Ge, T. H. Lee and G. Zhu, "Genetic-algorithm tuning of a Lyapunov-based controllers: an application to a single-link flexible robot system," *IEEE Trans. Ind. Elect.*, vol. 43, no. 5, pp. 567-574, 1996.

[22] R. J. Wai and M. C. Lee, "Intelligent Optimal control of single-link flexible robot arm," *IEEE Trans. Ind. Elect.*, vol. 51, no. 1, pp. 201-220, 2004.

[23] I. A. Mahmood, S. O. R. Moheiman and B. Bhikkaji, "Precise tip positioning of a flexible manipulator using resonant control," *IEEE/ASME Trans. Mechatr.*, vol. 13, no. 2, pp. 180-186, 2008.

[24] K. P. Liu, W.You and Y. C. Li, "Combining a feedback linearization approach with input shaping for flexible manipulator control" *Proc. 2nd Int. Conf. Mach. Learn. and Cybern.* 2003.

[25] M. A. Ahmad, Z. Mohamed and N. Hambali, "Dynamic Modeling of a Two-link Flexible Manipulator System Incorporating Payload," *IEEE Conf. Ind. Elect. Appl.*, pp. 96-101, 2008.

[26] *2-DOF serial flexible link robot,* Reference manual, Quanser.

[27] K. M. Passino, "Bacteria foraging optimization," *Int. J. Swarm Intellig. Resear.*, vol. 1, pp. 1-16, 2010.

[28] R. H. Cannon Jr. and E. Schmitz, "Initial experiments on the end-point control of a flexible one-link robot," *Int. J. Robot Res*, vol. 3, no. 3, 1984.

[29] C. M. Oakley and R. H. Canon Jr., "Initial experiments of the control of a two-link manipulator with a very flexible forearm," *American Contr. Confer.*, 1988.

[30] D. H. Kim, A. Abraham and J. H. Cho, "A hybrid genetic algorithm and bacteria foraging approach for global optimization," *Int. J. Infor. Science.*, vol. 177, pp. 3918-1937, 2007.

[31] J. S. R. Jang, C. T. Sun and E. Mizutani, *Neuro-fuzzy and soft computing, A computational approach to learning and machine intelligence.* Prentice Hall, New Jersey, 1997.